

Certifying Global Optimality of Graph Cuts via Semidefinite Relaxation: A Performance Guarantee for Spectral Clustering

Shuyang Ling* and Thomas Strohmer†

July 2, 2018

Abstract

Spectral clustering has become one of the most widely used clustering techniques when the structure of the individual clusters is non-convex or highly anisotropic. Yet, despite its immense popularity, there exists fairly little theory about performance guarantees for spectral clustering. This issue is partly due to the fact that spectral clustering typically involves two steps which complicated its theoretical analysis: first, the eigenvectors of the associated graph Laplacian are used to embed the dataset, and second, k-means clustering algorithm is applied to the embedded dataset to get the labels. This paper is devoted to the theoretical foundations of spectral clustering and graph cuts. We consider a convex relaxation of graph cuts, namely ratio cuts and normalized cuts, that makes the usual two-step approach of spectral clustering obsolete and at the same time gives rise to a rigorous theoretical analysis of graph cuts and spectral clustering. We derive deterministic bounds for successful spectral clustering via a *spectral proximity condition* that naturally depends on the algebraic connectivity of each cluster and the inter-cluster connectivity. Moreover, we demonstrate by means of some popular examples that our bounds can achieve near-optimality. Our findings are also fundamental for the theoretical understanding of kernel k-means. Numerical simulations confirm and complement our analysis.

1 Introduction

Organizing data into meaningful groups is one of the most fundamental tasks in data analysis and machine learning [26, 28]. K-means is probably the most well known and most widely used clustering method [33, 6, 26] in unsupervised learning. Yet, its performance is severely limited by two obstacles: (i) The k-means objective function is non-convex and finding its actual minimum is computationally hard; (ii) k-means operates under the tacit assumption that individual clusters lie within convex boundaries, and in addition are reasonably isotropic or widely separated. To address the first obstacle, heuristics such as Lloyd’s algorithm [33], are usually employed in an attempt to compute the solution in a numerically efficient manner. The second obstacle is more severe and independent of the actual algorithm used to find the objective function’s minimum.

Spectral clustering has arguably become the most popular clustering technique when the structure of the individual clusters is non-convex and/or highly anisotropic [47, 11, 35]. The spectral clustering algorithm typically involves two steps: (i) Laplacian eigenmaps: construct a similarity graph from the data and the eigenvectors of the associated graph Laplacian are used to embed the dataset into the feature space; (ii) rounding procedure: k-means is applied to the embedded dataset to obtain the clustering. As pointed out in [47], the immense success of spectral clustering lies in its flexibility to deal with data of various shapes and complicated geometry, mainly due to the Laplacian eigenmap based embedding prior to the k-means procedure. Thus

*Courant Institute of Mathematical Sciences, New York University (Email: sling@cims.nyu.edu).

†Department of Mathematics, University of California at Davis (Email: strohmer@math.ucdavis.edu).

‡T. Strohmer acknowledges partial support from the NSF via grants DMS 1620455 and DMS 1737943.

spectral clustering is also regarded as a variant of kernel k-means [21]. However, despite its enormous popularity and success, our theoretical understanding of the performance of spectral clustering is still rather vague. While there is vast empirical evidence of clustering examples in which e.g. spectral clustering by far outperforms k-means, there exists little rigorous theoretical analysis—even for very simple cases—that would prove the superiority of spectral clustering, partly due to the two-step procedure which complicates its theoretical analysis.

This paper is devoted to the theoretical foundations of spectral clustering and graph cuts. To begin with, we look at spectral clustering from a graph cut point of view and quickly review the state-of-the-art results which suggest to some extent why spectral clustering works. The basic intuition behind data clustering is to partition points into different groups based on their similarity. A partition of the data points always corresponds to a graph cut of the associated adjacency/similarity matrix. From the perspective of graph cuts, instead of computing the minimal graph cuts to obtain the data clustering, it is preferable to find a graph cut such that the sizes of all clusters are balanced and the inter-cluster connectivity is minimized. This is made possible by considering minimal ratio cuts and normalized cuts, which represent a traditional problem in graph theory [14, 5]. Those problems arise in a diverse range of applications besides spectral clustering, including community detection [1, 3, 4], computer vision and image segmentation [38]. While finding the optimal balanced graph cuts is a computationally hard problem in general, significant progress have been made to relax this problem by linking it to the spectra of the associated Laplacian matrix. This link immediately leads to spectral graph theory [17] which makes a great impact on many branches of mathematics and computer sciences. The two-step spectral clustering algorithm can be derived via graph ratio cuts [10, 11, 47, 25] and normalized cuts [35, 21, 38], which in turn are connected to graph Laplacian and normalized graph Laplacian, respectively.

The rather limited existing theory on spectral clustering is based on plain matrix perturbation analysis [47, 41, 20] especially via the famous Davis-Kahan theorem. The main reasoning behind perturbation analysis relies on the (unrealistic) assumption that if all underlying clusters on the graph are disconnected from one another, the eigenvectors of graph Laplacian with respect to the first few smallest eigenvalues are exactly indicator vectors which identify the data labels automatically. In the case when the eigenvectors are not exactly the indicator vectors (i.e., when the graph is connected), the perturbation argument fails to give the exact clustering and thus k-means is needed to perform the “rounding” procedure. Therefore, the perturbation argument, despite its simplicity, does not yield any optimality bounds that would establish under which conditions spectral clustering will succeed or fail to provide correct clustering.

Another direction of the state-of-the-art mathematical theories concentrates on spectral clustering for random data generative model especially for stochastic block model in [37, 30]. With the help of randomness, the performance bounds (such as misclassification rate) of the two-step spectral clustering algorithm are derived in [37] and the consistency of spectral clustering is given in [30]. Yet another related line of research focuses on understanding the convergence of the graph Laplacian associated with random samples to the Laplace-Beltrami operator on Riemannian manifolds [48, 11, 12, 39, 40, 43, 44]. Those excellent works establish a rigorous bridge between the discrete graph Laplacian and its continuous counterpart Laplace-Beltrami operator on the manifold [22].

While all the previous works are inspirational and illuminating, the key question is not fully addressed: under what type of conditions is spectral clustering able to identify the planted underlying partition exactly? More generally, how to certify a graph cut as the global optimum of ratio cuts or normalized cuts by using only the spectral properties of the (either normalized or unnormalized) graph Laplacian?

In this paper we answer these fundamental theoretical questions by taking a different approach, namely via considering convex relaxations of ratio cuts and normalized cuts, which solve spectral clustering as a special case (which may at first sound like a tautology, since spectral clustering in itself can be obtained as a relaxation of graph cuts). Our framework makes the standard two-step spectral clustering approach obsolete and at the same time gives rise to

a rigorous theoretical analysis. We derive *deterministic* bounds under which our semidefinite programming (SDP) relaxation of spectral clustering will produce the correct planted clusters. One highlighted feature of our result is that no assumption is imposed about the underlying probability distribution governing the data. Moreover, our theory serves as a simple criterion to certify if a graph cut is globally optimal under either ratio cuts or normalized cuts. The guarantees depend on a *spectral proximity condition*, a deterministic condition that encodes the algebraic connectivity of each cluster (the Fiedler eigenvalue of the graph Laplacian) and the inter-cluster connectivity in the case of ratio cuts and graph Laplacian. For the normalized cuts and normalized graph Laplacian, the guarantees have an intuitive probabilistic interpretation from a random walk point of view. Our bounds can be seen as a kernel-space analog of the well-known (Euclidean-space) proximity condition appearing in the theoretical analysis of k-means [29, 8, 32]. Furthermore, we demonstrate by means of simple, often used examples, that our theoretical framework can provide nearly optimal performance bounds for SDP spectral clustering.

Our approach is inspired by recent progress regarding the convex relaxation of k-means [36, 7, 27, 32] and follows the “Relax, no need to round”-paradigm. Note however, while the convex relaxation of k-means in [7, 27, 32] can provide a theoretical analysis concerning a successful computation of the optimal solution to the k-means objective function, it cannot overcome the fundamental limitations of the k-means objective function itself vis-a-vis nonconvex and anisotropic clusters. One attempt to address the latter shortcomings of k-means consists in replacing the Euclidean distance with a kernel function, leading to the aptly named kernel k-means algorithm [21, 50]. One can interpret the SDP spectral clustering framework derived in the current paper as an extension of the theoretical analysis of the convex relaxation k-means approach in [7, 32] to kernel k-means. Moreover, due to the natural connection between graph Laplacians and diffusion maps [19], our paper also sheds light on our theoretical understanding of diffusion map based data organization. Finally, we would like to acknowledge being influenced by the recent progress on the convex relaxation of community detection under stochastic block model [2, 9, 1, 3, 4, 51] in which the adjacency matrix is a binary random matrix. In fact, community detection problem can be viewed as an example of graph cuts problem on random graphs and hence our approach shares certain similarities with these previous works to some extent. However, as pointed out previously, our theoretic framework is significantly different from the existing literature since our theory does not assume any randomness as prior information and thus applies to more general settings besides community detection problem.

1.1 Organization of our paper

This paper is organized as follows. In Section 2 we review the basics of spectral clustering, motivated by both ratio cuts and normalized cuts. The proposed semidefinite relaxation of spectral clustering and our main theorems are presented in Section 3. We then demonstrate the near-optimality of the theoretical bounds by means of simple, well-known examples, see Section 4, and propose two open problems. Section 5 is devoted to numerical experiments that illustrate and complement the theoretical analysis. Finally, the proofs of our results can be found in Section 6.

1.2 Notation

For a vector z , we denote by $\|z\|$ its Euclidean norm and by $\|z\|_\infty$ the maximum of the absolute values of its components. For a matrix Z , we denote by $Z^{(a,b)}$ the (a,b) -block of Z (the size of the block $Z^{(a,b)}$ will be clear from the context) and by Z^\top the transpose of Z . Furthermore, $\|Z\|$ is the operator norm, $\|Z\|_F$ is its Frobenius norm, and $\|Z\|_\infty := \max_i \sum_j |Z_{ij}|$ is the matrix infinity norm. We define $\lambda_l(Z)$ to be the l -th smallest eigenvalue of Z . Given two matrices $Z, Y \in \mathbb{R}^{m \times n}$, we let $\langle Z, Y \rangle$ be the canonical inner product of Z and Y , i.e., $\langle Z, Y \rangle = \text{Tr}(Z^\top Y)$. For a vector z , we define $\text{diag}(z)$ to be a diagonal matrix whose diagonal entries consist of z . For a scalar z , we let $\lfloor z \rfloor$ be the largest integer smaller than z ; and for two scalars z and y , we say $z \gtrsim y$ if there exists two positive absolute constants such that $c_1 z \leq y \leq c_2 z$.

The vector $\mathbf{1}_m$ represents the $m \times 1$ vector with all entries equal to 1, $J_{m \times n} = \mathbf{1}_m \mathbf{1}_n^\top$ is the $m \times n$ “all-1” matrix, and I_n is the $n \times n$ identity matrix. We say $Z \succeq Y$ if $Z - Y \succeq 0$, i.e., $Z - Y$ is positive semidefinite, and $Z \geq Y$ if every entry of $Z - Y$ is nonnegative, i.e., $Z_{ij} - Y_{ij} \geq 0$. Finally, \mathcal{S}_n is the set of $n \times n$ symmetric matrices, \mathcal{S}_n^+ is the set of $n \times n$ symmetric positive semidefinite matrices, and $\mathbb{R}_+^{n \times n}$ denotes the set of all $n \times n$ nonnegative matrices.

2 Spectral clustering and graph cuts

Spectral clustering can be understood from the perspective of graph cuts. Here, we give a short introduction to spectral clustering and spectral graph theory. The interested readers may refer to the excellent review [47] for more details about spectral clustering and its variations. Spectral clustering is based on a similarity graph constructed from a given set of data points $\{x_i\}_{i=1}^N$ whose vertices correspond to data and edges are assigned a weight which encodes the similarity between any pair of data points, i.e., if x_i and x_j are close with respect to some similarity measure, then a larger weight is assigned to the edge (i, j) . Once the graph is obtained, one can compute the graph Laplacian, either normalized or unnormalized, and get the eigenvectors of the graph Laplacian to embed the data, followed by k-means or other rounding procedures to obtain the final clustering outcome. We refer the reader to [10, 11, 47, 25] for spectral clustering based on the unnormalized graph Laplacian and [35, 21, 38] for the normalized version.

2.1 A short tour of spectral clustering

We introduce the basics in spectral graph theory such as several versions of graph Laplacian which will be used later, and also the standard algorithms of spectral clustering. The first step of spectral clustering is to design the similarity matrix based on the data points. A well-known way to construct such a graph is to employ a non-negative, even kernel function $\Phi_\sigma(x, y)$ where σ determines the size of the neighborhood. Sometimes we call σ the bandwidth. A common choice for kernel function is of the following form,

$$\Phi_\sigma(x, y) = \Phi\left(\frac{\|x - y\|}{\sigma}\right),$$

where $\Phi(t)$ is a decreasing function of t . Typical examples for Φ include:

- $\Phi(t) = 1_{\{t \leq 1\}}$ which connects points if their pairwise distance is smaller than σ . This graph is known as σ -neighborhood graph and is more likely to be disconnected if some points are isolated.
- $\Phi(t) = e^{-\frac{t^2}{2}}$, the heat kernel. The resulting similarity matrix is a weighted complete graph. This kernel is also related to the diffusion process on the graph. The heat kernel is probably the most widely used kernel in connection with spectral clustering and graph cuts.

Suppose we have k planted clusters and the a -th cluster Γ_a has n_a data points, i.e., $|\Gamma_a| = n_a$. The data may not necessarily be linearly separable. Given a certain kernel $\Phi(\cdot)$, we denote the similarity matrix between cluster Γ_a and cluster Γ_b via

$$W_{ij}^{(a,b)} := \Phi\left(\frac{\|x_{a,i} - x_{b,j}\|}{\sigma}\right), \quad W^{(a,b)} \in \mathbb{R}^{n_a \times n_b}, \quad (2.1)$$

where $x_{a,i}$ is the i -th point in Γ_a . A particularly popular choice is the heat kernel, in which case W takes the form

$$W_{ij}^{(a,b)} := e^{-\frac{\|x_{a,i} - x_{b,j}\|^2}{2\sigma^2}}. \quad (2.2)$$

The total number of data points is $N = \sum_{a=1}^k n_a$. Without loss of generality we assume that the vertices are ordered according to the clusters they are associated with, i.e., lexicographical

order for $\{x_{a,i}\}_{1 \leq i \leq n_a, 1 \leq a \leq k}$. Hence, by combining all pairs of clusters, the full weight matrix becomes

$$W := \begin{bmatrix} W^{(1,1)} & W^{(1,2)} & \dots & W^{(1,k)} \\ W^{(2,1)} & W^{(2,2)} & \dots & W^{(2,k)} \\ \vdots & \vdots & \ddots & \vdots \\ W^{(k,1)} & W^{(k,2)} & \dots & W^{(k,k)} \end{bmatrix} \in \mathbb{R}^{N \times N}.$$

From now on, we let w_{ij} be the (i, j) entry of the weight matrix W and use $W_{ij}^{(a,b)}$ specifically for the (i, j) entry in the (a, b) block of W . Given the full weight matrix W , the degree of vertex i is $d_i = \sum_{j=1}^N w_{ij}$ and the associated degree matrix is

$$D := \text{diag}(W1_N)$$

where D is an $N \times N$ diagonal matrix with $\{d_i\}_{i=1}^N$ on the diagonal. We define the unnormalized graph Laplacian for the weight matrix W as

$$L := D - W \quad (2.3)$$

and the symmetric normalized graph Laplacian as

$$L_{\text{sym}} := I_N - D^{-\frac{1}{2}} W D^{-\frac{1}{2}} = D^{-\frac{1}{2}} L D^{-\frac{1}{2}}. \quad (2.4)$$

It is a simple exercise to verify that the quadratic form of L satisfies

$$v^\top L v = \sum_{1 \leq i < j \leq N} w_{ij} (v_i - v_j)^2 \quad (2.5)$$

where v_i is the i -th entry of v .

We also define

$$P := D^{-1} W, \quad L_{\text{rw}} := I_N - P \quad (2.6)$$

where the row sums of P are all equal to 1 and thus P defines a Markov transition matrix on the graph; L_{rw} is called random walk normalized Laplacian. Here $P_{ij} = \frac{w_{ij}}{d_i}$, the (i, j) entry of P , denotes the probability of a random walk starting from vertex i and moving to the vertex j in the next step.

For later use, we define a set of matrices with subscript “iso” which capture the within-cluster information. We denote the “isolated” weight matrix by W_{iso} that excludes the edges between different clusters, i.e.,

$$W_{\text{iso}} := \begin{bmatrix} W^{(1,1)} & 0 & \dots & 0 \\ 0 & W^{(2,2)} & \dots & 0 \\ \vdots & \vdots & \ddots & \vdots \\ 0 & 0 & \dots & W^{(k,k)} \end{bmatrix},$$

and the corresponding degree matrix

$$D_{\text{iso}} := \text{diag}(W_{\text{iso}}1_N).$$

The unnormalized graph Laplacian associated with W_{iso} is

$$L_{\text{iso}} := D_{\text{iso}} - W_{\text{iso}}. \quad (2.7)$$

We also define the random walk normalized Laplacian and Markov transition matrix for W_{iso} as

$$P_{\text{iso}} := D_{\text{iso}}^{-1} W_{\text{iso}}, \quad L_{\text{rw,iso}} := I_N - D_{\text{iso}}^{-1} W_{\text{iso}} \quad (2.8)$$

where P_{iso} and $L_{\text{rw,iso}}$ are block-diagonal matrices.

The following four matrices with subscript “ δ ” are used to measure the inter-cluster connectivity, namely,

$$\begin{aligned} W_\delta &:= W - W_{\text{iso}}, \\ D_\delta &:= D - D_{\text{iso}} = \text{diag}((W - W_{\text{iso}})1_N), \\ P_\delta &:= D^{-1}W_\delta = P - D^{-1}W_{\text{iso}}, \\ L_\delta &:= L - L_{\text{iso}} = D_\delta - W_\delta. \end{aligned} \tag{2.9}$$

From the definition above, we can see that W_δ and P_δ are the off-diagonal blocks of W and P respectively, and D_δ is a diagonal matrix whose diagonal entries equal the row sum of W_δ . These three matrices contain information about the inter-cluster connectivity.

We would like to point out that matrices with subscripts “iso” or “ δ ” are *depending* on the underlying partition $\{\Gamma_l\}_{l=1}^k$. So far, we also have seen graph Laplacian of three different weight matrices, i.e., L , L_{iso} , and L_δ , which are all positive semidefinite matrices because they are diagonally dominant and also can be seen from (2.5), and moreover the constant vector 1_N is in the null space. As long as a graph is connected, its corresponding graph Laplacian has a positive second smallest eigenvalue, cf. [17]. Moreover, the dimension of the nullspace of the graph Laplacian equals the number of connected components. Therefore, if all edge weights satisfy $w_{ij} > 0$ (which is possible if e.g. the Gaussian kernel is used), we have

$$\lambda_2(L) > 0, \quad \lambda_k(L_{\text{iso}}) = 0, \quad \lambda_{k+1}(L_{\text{iso}}) = \min_{1 \leq a \leq k} \lambda_2(L_{\text{iso}}^{(a,a)}) > 0,$$

because L_{iso} has k diagonal blocks and each one corresponds to a connected subgraph. Moreover, the nullspace of L_{iso} is spanned by k indicator vectors in \mathbb{R}^N , i.e., the columns of U_{iso} ,

$$U_{\text{iso}} := \begin{bmatrix} \frac{1}{\sqrt{n_1}}1_{n_1} & 0 & \cdots & 0 \\ 0 & \frac{1}{\sqrt{n_2}}1_{n_2} & \cdots & 0 \\ \vdots & \vdots & \ddots & \vdots \\ 0 & 0 & \cdots & \frac{1}{\sqrt{n_k}}1_{n_k} \end{bmatrix} \in \mathbb{R}^{N \times k}, \quad U_{\text{iso}}^\top U_{\text{iso}} = I_k.$$

Assume for the moment that the original data set has k clusters *and* that the graph constructed from the data has k connected components. In this case L will be a true block-diagonal matrix (after necessary permutations), it will have an eigenvalue 0 with multiplicity k and the corresponding eigenvectors will be indicator vectors that represent cluster membership of the data [47].

However, since initially we are *not* given the graph, but the data, we would have to assume that we know the cluster membership already a priori to be able to chose the ideal kernel that would then yield a graph with exactly k connected components. Since this is a futile assumption, L will *never* be an exact block-diagonal matrix, which in turn implies that the relevant eigenvectors will not be indicator vectors that represent cluster membership. Hence, standard spectral clustering essentially *always* necessitates a second step. This step may consist in rounding the eigenvectors to indicator vectors or, more commonly, in applying a method like k-means to the embedded data set.

We summarize the two most frequently used versions of spectral clustering algorithms in Algorithm 1 and 2 which use unnormalized and normalized graph Laplacian respectively.

In the Step 4 of Algorithm 2, one uses $D^{-\frac{1}{2}}U$ instead of U , which differs from Algorithm 1. This is to ensure that $D^{-\frac{1}{2}}U$ consists of k indicator vectors when the graph has k connected components and L_{sym} is a block-diagonal matrix.

Despite the tremendous success of spectral clustering in applications, its theoretical understanding is still far from satisfactory. Some theoretical justification for spectral clustering has been built on basic perturbation theory, by considering L as the sum of the block-diagonal matrix L_{iso} and the perturbation term L_δ , cf [35]. One can then invoke the Davis-Kahan theorem [20], which bounds the difference between eigenspaces of symmetric matrices under perturbations.

Algorithm 1 Unnormalized spectral clustering

- 1: **Input:** Given the number of clusters k and a dataset $\{x_i\}_{i=1}^N$, construct the similarity matrix W from $\{x_i\}_{i=1}^N$.
 - 2: Compute the unnormalized graph Laplacian $L = D - W$.
 - 3: Compute the eigenvectors $\{u_l\}_{l=1}^k$ of L w.r.t. the smallest k eigenvalues.
 - 4: Let $U = [u_1, u_2, \dots, u_k] \in \mathbb{R}^{N \times k}$. Perform k -means clustering on the rows of U by using Lloyd's algorithm.
 - 5: Obtain the partition based on the outcome of k -means.
-

Algorithm 2 Normalized spectral clustering

- 1: **Input:** Given the number of clusters k and a dataset $\{x_i\}_{i=1}^N$, construct the similarity matrix W from $\{x_i\}_{i=1}^N$.
 - 2: Compute the normalized graph Laplacian $L_{\text{sym}} = I_N - D^{-\frac{1}{2}} W D^{-\frac{1}{2}}$.
 - 3: Compute the eigenvectors $\{u_l\}_{l=1}^k$ of L_{sym} w.r.t. the smallest k eigenvalues.
 - 4: Let $U = [u_1, u_2, \dots, u_k] \in \mathbb{R}^{N \times k}$. Perform k -means clustering on the rows of $D^{-\frac{1}{2}} U$ by using Lloyd's algorithm.
 - 5: Obtain the partition based on the outcome of k -means.
-

Then an error bound is obtained between U and U_{iso} in terms of $\|L_\delta\|$ (or $\|L_\delta\|_F$) where U and U_{iso} are the eigenvectors w.r.t. the smallest k eigenvalues of L and L_{iso} respectively. However, the statements obtained with this line of reasoning have been more of a qualitative nature since the error bound between U and U_{iso} does not immediately reflect the quality of clustering, partly due to the difficulty of analyzing the performance of k -means applied to U . Thus, the perturbation arguments have not yet provided explicit conditions under which spectral clustering would succeed or fail, not to speak of bounds that are anywhere near optimality, or even theorems that would just prove that spectral clustering does actually outperform k -means in simple, often-used examples when promoting spectral clustering.

2.2 Understanding spectral clustering via graph cuts

Graph partitioning provides a powerful tool of understanding and deriving spectral clustering; it also becomes the foundation of this work. Given a graph, one wants to divide it into several pieces such that the inter-cluster connectivity is small and each cluster is well connected within itself. However, only based on this criterion, this does usually not give satisfactory results since one single vertex may likely be treated as one cluster. As a consequence, it is usually preferable to have clusters whose sizes are relatively large enough, i.e., clusters of very small size should be avoided. To realize that, one uses ratio cuts [47, 25] and normalized cuts [21, 38] to ensure the balancedness of cluster sizes. Hence, we now discuss ratio cuts and normalized cuts, and their corresponding spectral relaxation. We also want to point out that the discussion about graph cuts applies to more *general* settings and spectral clustering is viewed to some extent as a special case of graph cuts.

Ratio cuts and their spectral relaxation

Given a disjoint partition $\{\Gamma_a\}_{a=1}^k$ such that $\sqcup_{a=1}^k \Gamma_a = [N] := \{1, \dots, N\}$, we define ratio cuts (RatioCut) as

$$\text{RatioCut}(\{\Gamma_a\}_{a=1}^k) := \sum_{a=1}^k \frac{\text{cut}(\Gamma_a, \Gamma_a^c)}{|\Gamma_a|}. \quad (2.10)$$

Here, the cut is defined as the weight sum of edges whose two ends are in different subsets,

$$\text{cut}(\Gamma, \Gamma^c) := \sum_{i \in \Gamma, j \in \Gamma^c} w_{ij} \quad (2.11)$$

where Γ is a subset of vertices and Γ^c is its complement. In fact, (2.11) can be neatly written in terms of the graph Laplacian L . By definition of L in (2.3), there holds

$$\text{cut}(\Gamma_a, \Gamma_a^c) := \sum_{i \in \Gamma_a, j \in \Gamma_a^c} w_{ij} = \langle L^{(a,a)}, 1_{|\Gamma_a|} 1_{|\Gamma_a|}^\top \rangle, \quad (2.12)$$

which follows from

$$\begin{aligned} \langle L^{(a,a)}, 1_{|\Gamma_a|} 1_{|\Gamma_a|}^\top \rangle &= \langle D^{(a,a)} - W^{(a,a)}, 1_{|\Gamma_a|} 1_{|\Gamma_a|}^\top \rangle = \sum_{l=1}^k 1_{|\Gamma_a|}^\top W^{(a,l)} 1_{|\Gamma_l|} - 1_{|\Gamma_a|}^\top W^{(a,a)} 1_{|\Gamma_a|} \\ &= \sum_{l \neq a} 1_{|\Gamma_a|}^\top W^{(a,l)} 1_{|\Gamma_l|} = \sum_{i \in \Gamma_a, j \in \Gamma_a^c} w_{ij}. \end{aligned}$$

Therefore, RatioCut is in fact the inner product between the graph Laplacian L and a block-diagonal matrix X_{rcut} ,

$$\text{RatioCut}(\{\Gamma_a\}_{a=1}^k) = \sum_{a=1}^k \frac{1}{|\Gamma_a|} \langle L^{(a,a)}, 1_{|\Gamma_a|} 1_{|\Gamma_a|}^\top \rangle = \langle L, X_{\text{rcut}} \rangle,$$

where

$$X_{\text{rcut}} := \sum_{a=1}^k \frac{1}{|\Gamma_a|} 1_{\Gamma_a} 1_{\Gamma_a}^\top = \text{blockdiag} \left(\frac{1}{|\Gamma_1|} 1_{|\Gamma_1|} 1_{|\Gamma_1|}^\top, \dots, \frac{1}{|\Gamma_k|} 1_{|\Gamma_k|} 1_{|\Gamma_k|}^\top \right) \in \mathbb{R}^{N \times N}, \quad (2.13)$$

and $1_{\Gamma_a}(\cdot)$ is an indicator vector which maps a vertex to a vector in \mathbb{R}^N via

$$1_{\Gamma_a}(l) = \begin{cases} 1, & l \in \Gamma_a, \\ 0, & l \notin \Gamma_a. \end{cases}$$

Obviously, by putting the cardinality of Γ_a in the denominator of (2.10), one can avoid small clusters and thus RatioCut is a more favorable criterion to conduct graph partition. However, minimizing RatioCut is an NP-hard problem [47]. Here we discuss one very popular and useful relaxation of RatioCut which relates the RatioCut problem to an eigenvalue problem.

From our previous discussion, we realize that to minimize RatioCut over all possible partitions $\{\Gamma_a\}_{a=1}^k$ of $[N]$, it suffices to minimize $\langle L, Z \rangle$ for all matrices Z as (2.13) which is essentially a positive semidefinite projection matrix. Spectral clustering is a relaxation by these two properties,

$$X_{\text{rcut}} = UU^\top, \quad U^\top U = I_k, \quad U \in \mathbb{R}^{N \times k}.$$

Therefore, one instead considers a simple matrix eigenvalue/eigenvector problem,

$$\min_{U \in \mathbb{R}^{N \times k}} \langle L, UU^\top \rangle \quad \text{s.t.} \quad U^\top U = I_k, \quad (2.14)$$

whose global minimizer is easily found via computing the eigenvectors w.r.t. the k smallest eigenvalues of the graph Laplacian L . Therefore, the Laplacian eigenmaps step of Algorithm 1 has a natural explanation via the spectral relaxation of RatioCut.

Normalized cuts and their spectral relaxation

The normalized cut (NCut) differs from RatioCut by using the volume to quantify the size of cluster Γ_l instead of the cardinality $|\Gamma_l|$. RatioCut and NCut behave similarly if each node of the graph has very similar degree, i.e., the graph is close to a regular graph. The NCut of a given partition $\{\Gamma_l\}_{l=1}^k$ is defined as

$$\text{NCut}(\{\Gamma_a\}_{a=1}^k) := \sum_{a=1}^k \frac{\text{cut}(\Gamma_a, \Gamma_a^c)}{\text{vol}(\Gamma_a)} \quad (2.15)$$

where the volume of Γ_a is defined as the sum of degrees of vertices in the subset Γ_a ,

$$\text{vol}(\Gamma_a) := \sum_{i \in \Gamma_a} d_i = \sum_{i \in \Gamma_a} \sum_{j=1}^N w_{ij}. \quad (2.16)$$

Just like the link between RatioCut and the graph Laplacian, we can relate (2.15) to the normalized Laplacian (2.4). By using (2.11), (2.12), and $\text{vol}(\Gamma_a) = \langle D, 1_{\Gamma_a} 1_{\Gamma_a}^\top \rangle = 1_{\Gamma_a}^\top D 1_{\Gamma_a}$, and then

$$\begin{aligned} \text{NCut}(\{\Gamma_a\}_{a=1}^k) &= \sum_{a=1}^k \frac{1_{\Gamma_a}^\top L 1_{\Gamma_a}}{1_{\Gamma_a}^\top D 1_{\Gamma_a}} = \sum_{a=1}^k \left\langle L, \frac{1_{\Gamma_a} 1_{\Gamma_a}^\top}{1_{\Gamma_a}^\top D 1_{\Gamma_a}} \right\rangle \\ &= \sum_{a=1}^k \left\langle D^{-\frac{1}{2}} L D^{-\frac{1}{2}}, \frac{D^{\frac{1}{2}} 1_{\Gamma_a} 1_{\Gamma_a}^\top D^{\frac{1}{2}}}{1_{\Gamma_a}^\top D 1_{\Gamma_a}} \right\rangle \\ &= \langle L_{\text{sym}}, X_{\text{ncut}} \rangle. \end{aligned}$$

Here L_{sym} is the normalized Laplacian in (2.4) and

$$X_{\text{ncut}} := \sum_{a=1}^k \frac{1}{1_{\Gamma_a}^\top D 1_{\Gamma_a}} D^{\frac{1}{2}} 1_{\Gamma_a} 1_{\Gamma_a}^\top D^{\frac{1}{2}}. \quad (2.17)$$

If we replace D with an identity matrix multiplied by a scalar, then X_{ncut} is equal to X_{rcut} .

Similar to RatioCut, minimizing RatioCut is an NP-hard problem and one can instead use the following convenient spectral relaxation,

$$\min_{U \in \mathbb{R}^{N \times k}} \langle L_{\text{sym}}, U U^\top \rangle, \quad \text{s.t.} \quad U^\top U = I_k, \quad (2.18)$$

because X_{ncut} in (2.17) is also a positive semidefinite orthogonal projection matrix and thus can be factorized into $X_{\text{ncut}} = U U^\top$ with $U^\top U = I_k$.

Although it is very convenient to compute the global minimizer U_{rcut} and U_{ncut} in (2.14) and (2.18) respectively, as mentioned earlier they unfortunately do not usually return the exact cluster membership, unless the graph has exactly k connected components. Suppose there are k connected components, then it is straightforward to verify

$$U_{\text{rcut}} = U_{\text{iso}}, \quad U_{\text{ncut}} = D^{\frac{1}{2}} U_{\text{iso}} (U_{\text{iso}}^\top D U_{\text{iso}})^{-\frac{1}{2}} \quad (2.19)$$

are the global minimizer of (2.14) and (2.18) respectively up to an orthogonal transformation. Then all columns of U_{rcut} and $D^{-\frac{1}{2}} U_{\text{ncut}}$ are indicator vectors and they imply the connected components automatically. However, in general, the minimizer U_{rcut} and $D^{-\frac{1}{2}} U_{\text{ncut}}$ are not in the form of (2.19) if the graph is connected. Thus, k-means, as a rounding procedure, is applied to U_{rcut} and $D^{-\frac{1}{2}} U_{\text{ncut}}$ to estimate the underlying clusters. Those observations lead to Algorithm 1 and 2, respectively.

3 SDP relaxation of graph cuts and main results

In this section, we propose semidefinite relaxation of spectral clustering for both ratio cuts and normalized cuts, and present the *spectral proximity condition*, which certifies the global optimality of a graph cut under either ratio cuts or normalized cuts. The spectral proximity condition is purely deterministic; it depends only on the within-cluster connectivity (algebraic connectivity of a graph) and inter-cluster connectivity. We then apply our results to spectral clustering, as a special case of graph cuts, and thus obtain the desired theoretical guarantees for spectral clustering.

3.1 Graph cuts via semidefinite programming

We add one more constraint to both programs, (2.14) and (2.18), and the so obtained modification results in the SDP relaxation of graph cuts.

SDP relaxation of RatioCut: Note that minimizing RatioCut is equivalent to minimizing $\langle L, Z \rangle$ over all matrices Z in the form of (2.13), which is a semidefinite block-diagonal orthogonal projection matrix up to a row/column permutation. Since this combinatorial optimization problem is NP-hard in nature, the idea of SDP relaxation in this context is to replace the feasible matrices in the form of (2.13) by a convex set which contains all such matrices as a proper subset. We first try to find out what properties matrices Z in the form of (2.13) have for any given partition:

1. Z is positive semidefinite, $Z \succeq 0$;
2. Z is nonnegative, $Z \geq 0$ entrywisely;
3. the constant vector is an eigenvector of Z which means $Z1_N = 1_N$;
4. the trace of Z equals k , i.e., $\text{Tr}(Z) = k$.

It is obvious that the first two conditions are convex, and both conditions 3) and 4) are linear. Therefore, instead of minimizing $\langle L, Z \rangle$ over all Z as in (2.13), we relax the originally combinatorial optimization by using the following convex relaxation:

$$\min_{Z \in \mathcal{S}_N} \langle L, Z \rangle \quad \text{s.t.} \quad Z \succeq 0, \quad Z \geq 0, \quad \text{Tr}(Z) = k, \quad Z1_N = 1_N. \quad (3.1)$$

In fact, if $U_{\text{rcut}} \in \mathbb{R}^{N \times k}$ is the solution to the spectral relaxation (2.14), then $\hat{Z} = U_{\text{rcut}} U_{\text{rcut}}^\top$ satisfies all the conditions in (3.1) except for the nonnegativity condition.

SDP relaxation of NCut: The partition matrix in (2.17) shares three properties with those in (2.13):

$$Z \succeq 0, \quad Z \geq 0, \quad \text{Tr}(Z) = k.$$

The only difference is the appearance of the term $D^{\frac{1}{2}}1_N$ instead of 1_N ,

$$ZD^{\frac{1}{2}}1_N = \sum_{a=1}^k \frac{1}{1_{\Gamma_a}^\top D 1_{\Gamma_a}} D^{\frac{1}{2}} 1_{\Gamma_a} 1_{\Gamma_a}^\top D 1_N = \sum_{a=1}^k \frac{1_{\Gamma_a}^\top D 1_N}{1_{\Gamma_a}^\top D 1_{\Gamma_a}} D^{\frac{1}{2}} 1_{\Gamma_a} = D^{\frac{1}{2}} 1_N.$$

As a result, the corresponding convex relaxation of normalized cuts is

$$\min_{Z \in \mathcal{S}_N} \langle L_{\text{sym}}, Z \rangle, \quad \text{s.t.} \quad Z \succeq 0, \quad Z \geq 0, \quad \text{Tr}(Z) = k, \quad ZD^{\frac{1}{2}}1_N = D^{\frac{1}{2}}1_N. \quad (3.2)$$

Similarly, we can also see that the main difference between (3.2) and (2.18) is the nonnegativity condition. We summarize our approach in Algorithm 3.

From a numerical viewpoint Algorithm 3 does not lend itself easily to an efficient implementation for large scale data clustering. The question of how to solve (3.1) and (3.2) in a computationally efficient manner is a topic for future research. In this paper our focus is on getting theoretical insights into the performance of graph cuts and spectral clustering. Define the ground truth partition matrix X as

$$X := \begin{cases} X_{\text{rcut}}, & \text{for RatioCut in (2.13),} \\ X_{\text{ncut}}, & \text{for NCut in (2.17).} \end{cases} \quad (3.3)$$

Thus, the key questions we need to address are:

Under which conditions does Algorithm 3 exactly recover the underlying partition X in (3.3)? Are these conditions approximately optimal?

Algorithm 3 SDP relaxation of spectral clustering: **RatioCut-SDP** and **NCut-SDP**

- 1: **Input:** Given a dataset $\{x_i\}_{i=1}^N$ and the number of clusters k , construct the weight matrix W from $\{x_i\}_{i=1}^N$.
- 2: Compute the unnormalized graph Laplacian $L = D - W$ or its normalized graph Laplacian $L_{\text{sym}} = I_N - D^{-\frac{1}{2}}WD^{-\frac{1}{2}}$.
- 3: Solve the following semidefinite programs:
 - a) **RatioCut-SDP:**

$$\hat{Z} := \operatorname{argmin}_{Z \in \mathcal{S}_N} \langle L, Z \rangle \quad \text{s.t.} \quad Z \succeq 0, \quad Z \geq 0, \quad \operatorname{Tr}(Z) = k, \quad Z1_N = 1_N.$$

- b) **NCut-SDP:**

$$\hat{Z} := \operatorname{argmin}_{Z \in \mathcal{S}_N} \langle L_{\text{sym}}, Z \rangle \quad \text{s.t.} \quad Z \succeq 0, \quad Z \geq 0, \quad \operatorname{Tr}(Z) = k, \quad ZD^{\frac{1}{2}}1_N = D^{\frac{1}{2}}1_N.$$

- 4: Obtain the cluster partitioning based on \hat{Z} .
-

As discussed above, the main difference of RatioCut-SDP and NCut-SDP from the spectral relaxation (2.14) and (2.18) comes from the nonnegativity constraint. We would like to see how this constraint in the SDP relaxation contributes to the final performance.

In fact, this relaxation is not entirely new. Xing and Jordan [50] proposed a very similar SDP relaxation for normalized k-cut by considering the nonnegativity constraint and applied the SDP relaxation to several datasets. Another closely related type of convex relaxation has originally been proposed by Peng and Wei for k-means-type clustering [36]. There, instead of L (or L_{sym}), one has a matrix containing the squared pairwise Euclidean distances between data points or a similarity matrix. In recent years, theoretical guarantees of the Peng-Wei relaxation have been derived for k-means [27, 34, 32, 42]. Furthermore, the Peng-Wei relaxation has been extended to community detection problems [51, 4]. Note that the presence of the graph Laplacian instead of an Euclidean distance matrix does not only substantially (and positively) affect the clustering performance, but it also significantly changes the proof strategy (and resulting conditions) in order to establish exact clustering guarantees.

3.2 Main theorems

Simple perturbation theory directly applied to the graph Laplacian so far has not led to competitive performance bounds. It either requires the futile assumption of a graph with properly disconnected components, or the results are merely of handwaving nature. While our analysis will also invoke perturbation theory at some stage, a crucial difference is that we get competitive and rigorous quantitative performance guarantees without imposing the unrealistic assumption of a disconnected graph.

Our performance bounds depend the balancedness of the underlying clusters and we define the ratio τ for this purpose,

$$\tau := \begin{cases} \frac{\max_l n_l}{\min_l n_l}, & \text{for RatioCut,} \\ \frac{\max_l \operatorname{vol}(\Gamma_l)}{\min_l \operatorname{vol}(\Gamma_l)}, & \text{for NCut.} \end{cases} \quad (3.4)$$

A large value of τ means that the dataset exhibits (some) clusters of very different size, while $\tau \approx 1$ means that all clusters are about the same size (or volume).

In the following theorem we give a natural condition, called *spectral proximity condition*, under which Algorithm 3 yields the correct clustering of the data. Both conditions in (3.5) and (3.6) can be interpreted as a kernel-space analog of the Euclidean-space proximity condition appearing in the theoretical analysis of k-means [29, 8, 32].

Theorem 3.1 (Spectral proximity condition for RatioCut-SDP). *The semidefinite relaxation (3.1) gives X_{rcut} in (2.13) as the unique global minimizer if the following spectral proximity condition holds*

$$\|D_\delta\| \leq \frac{\lambda_{k+1}(L_{\text{iso}})}{2(k-1)(\tau+1)+3}, \quad (3.5)$$

where $\lambda_{k+1}(L_{\text{iso}})$ is the $(k+1)$ -th smallest eigenvalue of the graph Laplacian L_{iso} defined in (2.7). Here $\lambda_{k+1}(L_{\text{iso}})$ satisfies

$$\lambda_{k+1}(L_{\text{iso}}) = \min_{1 \leq a \leq k} \lambda_2(L_{\text{iso}}^{(a,a)})$$

where $\lambda_2(L_{\text{iso}}^{(a,a)})$ is the second smallest eigenvalue of graph Laplacian w.r.t. the a -th cluster.

As pointed out in [35], the success of spectral clustering depends on the within-cluster connectivity (algebraic connectivity, which is captured by $\lambda_2(L_{\text{iso}}^{(a,a)})$), as well as the “noise” $\|D_\delta\|$ which measures the inter-cluster connectivity. If the latter quantity is close to 0, spectral clustering should succeed, because the eigenspace of L w.r.t. the smallest k eigenvalues will be close to U_{iso} . Our condition (3.5) makes the intuition behind [35] precise. Note that the operator norm of D_δ equals

$$\|D_\delta\| = \|W_\delta 1_N\|_\infty = \max_{1 \leq a \leq k} \max_{i \in \Gamma_a} \sum_{j \notin \Gamma_a} w_{ij},$$

which quantifies the maximal inter-cluster degree. If this quantity is smaller than the within-cluster connectivity $\lambda_2(L_{\text{iso}}^{(a,a)})$ (modulo a factor that depends on the number of clusters and the balancedness of the clusters), then convex relaxation of RatioCut is able to find the underlying partition *exactly*.

For the SDP relaxation of the normalized cuts, we have the following theorem under slightly different conditions.

Theorem 3.2 (Spectral proximity condition for NCut-SDP). *The semidefinite relaxation (3.2) gives X_{ncut} in (2.17) as the unique global minimizer if the following spectral proximity condition holds*

$$\frac{\|P_\delta\|_\infty}{1 - \|P_\delta\|_\infty} \leq \frac{\lambda_{k+1}(L_{\text{rw,iso}})}{2(k-1)(\tau+1)+3}, \quad (3.6)$$

where $\lambda_{k+1}(L_{\text{rw,iso}})$ is the $(k+1)$ -th smallest eigenvalue of $L_{\text{rw,iso}}$. Moreover, $\lambda_{k+1}(L_{\text{rw,iso}})$ satisfies

$$\lambda_{k+1}(L_{\text{rw,iso}}) = \min_{1 \leq a \leq k} \lambda_2(L_{\text{rw,iso}}^{(a,a)}) = \min_{1 \leq a \leq k} \lambda_2(I_{n_a} - P_{\text{iso}}^{(a,a)})$$

due to the block-diagonal structure of $L_{\text{rw,iso}}$ and P_{iso} in (2.8).

The condition (3.6) has a probabilistic interpretation. Note that $P = D^{-1}W$ is a Markov transition matrix in (2.6), P_δ is the off-diagonal blocks of P in (2.9), and $\|P_\delta\|_\infty$ is the maximal probability of a random walker leaving its own cluster after one step. Thus, if the left hand side in (3.6) is small, for example less than 1, it means a random walker starting from *any* node is *more* likely to stay in its own cluster than leave it after one step, and vice versa. In other words, the left hand side of (3.6) characterizes the strength of inter-cluster connectivity. On the other hand, the right hand of (3.6) equals $\lambda_2(I_{n_a} - P_{\text{iso}}^{(a,a)})$ which is the eigengap¹ of Markov transition matrix for the random walk restricted on the a -th cluster. It is well known that a larger eigengap implies stronger connectivity of each individual cluster as well as faster mixing time [31] of the Markov chain defined on a -th cluster. The matrix $P = D^{-1}W$ plays also a central role in the diffusion map framework [18]. Thus, our approach paves the way to derive theoretical guarantees for clustering based on diffusion maps.

¹The gap means the difference between the first and the second largest eigenvalue of the Markov transition matrix.

While the convex relaxation approach to k-means leads to conditions that are directly expressible as separation conditions between clusters in terms of Euclidean distances, this is not the case in Theorem 3.1 and Theorem 3.2, nor should one expect this for general clusters. After all, the whole point of resorting to spectral clustering is that one may have to cluster datasets which are not neatly separated by the Euclidean distance, see e.g. the example in Section 4.1.

Theorems 3.1 and 3.2 do not only apply to spectral clustering but also to graph cuts. The attentive reader may have noticed that Theorems 3.1 and 3.2 do not rely on any information of a data generative model of the underlying clusters or on the choice of kernel function $\Phi(\cdot)$. Instead, the assumptions in both theorems are purely algebraic conditions which only depend on the spectral properties of the graph Laplacian. Thus these two results not only apply to spectral clustering but also to general graph partition problems. Suppose we have an undirected graph with weight matrix W (not necessarily in the form of (2.1)) and compute the corresponding graph Laplacian L . We try to partition the graph into several subgraphs such that RatioCut or NCut is minimized. Then if a given partition $\{\Gamma_a\}_{a=1}^k$ (any partition $\{\Gamma_a\}_{a=1}^k$ gives rise to W_{iso} and L_{iso}) satisfies (3.5) or (3.6), then $\{\Gamma_a\}_{a=1}^k$ is the only global minimizer of RatioCut or NCut respectively. Moreover, this partition can be found via the SDP relaxation (3.1) and (3.2).

As a result, Theorem 3.1 and 3.2 also yield performance bounds for successful community detection under stochastic block model with multiple communities [1, 3, 4, 9] because the community detection problem is an important example of graph cuts problem. We apply Theorem 3.1 to stochastic block model and present the performance bound in Section 4.4. However, the bounds obtained here will not be as tight as those found in the state-of-the-art literature (by a factor of constant). The main reason is due to the fact that our derivation of Theorem 3.1 does not rely on randomness. Since our theorem does not make use of the full information (namely the randomness) present in the stochastic block model, it is not surprising that it will give somewhat looser bounds.

4 Near-optimality of spectral proximity condition

It is natural to ask whether the semidefinite relaxation of spectral clustering can achieve better results than ordinary k-means. In this section we will demonstrate by means of concrete examples that our framework can indeed achieve near-optimal clustering performance. The first two examples are deterministic examples in which the data are placed on two concentric circles or two parallel lines. Those two examples are often cited to demonstrate better performance of spectral clustering over that of ordinary k-means. However, to the best of our knowledge, rigorous theoretic performance analysis of spectral clustering on these examples is still lacking. We will apply Theorem 3.1 to show that the SDP relaxation of spectral clustering will work with guarantees while, on the other hand, k-means fails.

The key ingredient to invoke Theorem 3.1 is the estimation of the second smallest eigenvalue of the graph Laplacian associated with each cluster. While we are able to show the estimation of this quantity for deterministic examples, it is more appealing to find out a framework to compute the algebraic connectivity of graph Laplacians with data generated from a probability distribution on a manifold. This is an important mathematical problem by itself and we will discuss it briefly in Section 4.3. In Section 4.4, we apply Theorem 3.1 to stochastic block model and compare our performance bound with the state-of-the-art results.

4.1 Two concentric circles

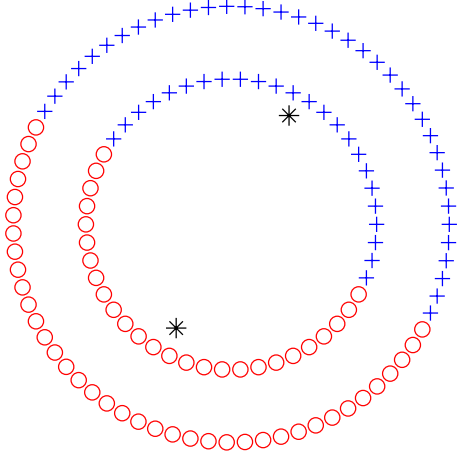
We first present an example in which k-means clustering obviously must fail, but spectral clustering is known to succeed empirically, cf. Figure 1. While this example is frequently used to motivate the use of spectral clustering, kernel k-means, or diffusion maps over standard k-means, so far this motivation was solely based on empirical evidence, since until now no theoretical guarantees have been given to justify it. We will give an explicit condition derived from Theorem 3.1 under which Algorithm 3 is provably able to recover the underlying clusters

exactly and in addition it can do so at a nearly minimal cluster separation, thereby putting this popular empirical example finally on firm theoretical ground.

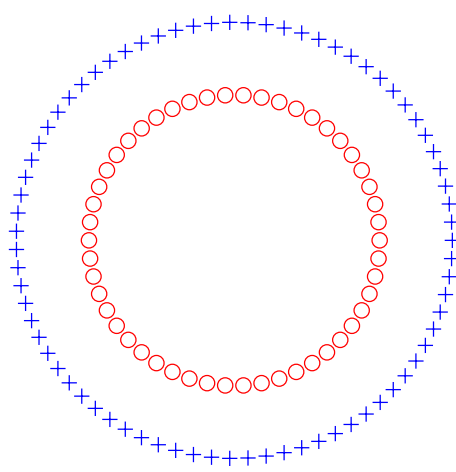
Suppose we have two circles centered at the origin. The data are equispaced on the circles, i.e.,

$$x_{1,i} = r_1 \begin{bmatrix} \cos(\frac{2\pi i}{n}) \\ \sin(\frac{2\pi i}{n}) \end{bmatrix}, \quad 1 \leq i \leq n; \quad x_{2,j} = r_2 \begin{bmatrix} \cos(\frac{2\pi j}{m}) \\ \sin(\frac{2\pi j}{m}) \end{bmatrix}, \quad 1 \leq j \leq m \quad (4.1)$$

where $m = \lfloor n\kappa \rfloor$ and $\kappa = \frac{r_2}{r_1} > 1$. The parameters are chosen so that the distance between adjacent points in each individual cluster is approximately $\frac{2\pi r_1}{n}$. In this example, we pick the Gaussian kernel $\Phi_\sigma(x, y) = e^{-\frac{\|x-y\|^2}{2\sigma^2}}$ to construct weight matrix and graph Laplacian.



(a) Result via Matlab's built-in k-means++ and “*” stands for the centroids of clusters.



(b) Result via SDP relaxation of spectral clustering

Figure 1: Two concentric circles with radii $r_1 = 1$ and $r_2 = \frac{3}{2}$, and $n = 50$ and $m = 75$. (a) If one performs Matlab's built-in kmeans++, the underlying clusters of the data will obviously not be extracted since two clusters are not linearly separable; (b) If one performs SDP relaxation of spectral clustering with bandwidth $\sigma = \frac{4}{n}$, the two circles are recovered exactly.

Theorem 4.1. *Let the data $\{x_i\}_{i=1}^{n+m}$ be given by $\{x_{1,i}\}_{i=1}^n \cup \{x_{2,i}\}_{i=1}^m$ as defined in (4.1) and let the ratio of the two radii be $\kappa = \frac{r_2}{r_1}$ and $\Delta := \frac{r_2 - r_1}{r_1} = \kappa - 1$. Let Φ be the heat kernel with σ chosen as follows*

$$\sigma^2 = \frac{16r_1^2\gamma}{n^2 \log(\frac{m}{2\pi})}.$$

Then Algorithm 3 recovers the underlying two clusters $\{x_{1,i}\}_{i=1}^n$ and $\{x_{2,i}\}_{i=1}^m$ exactly if the separation Δ satisfies

$$\Delta \geq \frac{4}{n} \sqrt{1 + 2\gamma \left(2 + \frac{\log(7\kappa m)}{\log(\frac{m}{2\pi})} \right)}. \quad (4.2)$$

To see that the separation Δ in Theorem 4.1 is $\tilde{\mathcal{O}}$ -optimal, assume w.l.o.g. $r_1 = 1$. In this case the minimum distance between points in the same circle is about $\frac{2\pi}{n}$. Therefore, we can only expect spectral clustering to recover the two circle clusters correctly if the minimum distance between points of different circles is larger than $\frac{2\pi}{n}$, i.e. $r_2 \geq 1 + \frac{2\pi}{n}$. Indeed, the condition in (4.2) shows that a separation $\Delta = \tilde{\mathcal{O}}(\frac{1}{n})$ suffices for successful recovery of the two clusters.

4.2 Two parallel lines

Here is another example showing the limitation of k-means, even though the two clusters are perfectly within convex boundaries. The issue here is that the two clusters are highly anisotropic,

which is a major problem for k-means².

Suppose the data points are distributed on two lines with separation Δ as illustrated in Figure 2,

$$x_{1,i} = \begin{bmatrix} -\frac{\Delta}{2} \\ \frac{i-1}{n-1} \end{bmatrix}, \quad x_{2,i} = \begin{bmatrix} \frac{\Delta}{2} \\ \frac{i-1}{n-1} \end{bmatrix}, \quad 1 \leq i \leq n, \quad (4.3)$$

where n is the number of data points on each time and there are $2n$ points in total.

We claim that if n is large and $\Delta < \frac{1}{2}$, the k-means optimal solution will not return the underlying partition, as suggested by the following calculations. For simplicity, we also assume n as an even number. If we set the cluster centers to be $c_1 = [-\frac{\Delta}{2} \ \frac{1}{2}]^\top$ and $c_2 = [\frac{\Delta}{2} \ \frac{1}{2}]^\top$, as the geometry suggests, then the k-means objective function value is

$$\Psi_n(c_1, c_2) = 2 \sum_{i=1}^n \left(\frac{i-1}{n-1} - \frac{1}{2} \right)^2 = \frac{n(2n-1)}{3(n-1)} - \frac{n}{2}$$

which follows from $\sum_{i=1}^n i^2 = \frac{n(n+1)(2n+1)}{6}$. As n goes to infinity, the average objective function value over $2n$ points becomes

$$\lim_{n \rightarrow \infty} \frac{\Psi_n(c_1, c_2)}{2n} = \frac{1}{3} - \frac{1}{4} = \frac{1}{12}.$$

However, if we pick the cluster centers as $c_1 = [0 \ \frac{n-2}{4(n-1)}]^\top$ and $c_2 = [0 \ \frac{3n-2}{4(n-1)}]^\top$, then

$$\Psi_n(c_1, c_2) = 4 \sum_{i=1}^{\frac{n}{2}} \left(\frac{\Delta^2}{4} + \left(\frac{i-1}{n-1} - \frac{n-2}{4(n-1)} \right)^2 \right) = \frac{n\Delta^2}{2} + \frac{n(n-2)}{6(n-1)} - \frac{n(n-2)^2}{8(n-1)^2}.$$

The limit of average objective function value in this case is

$$\lim_{n \rightarrow \infty} \frac{\Psi_n(c_1, c_2)}{2n} = \frac{\Delta^2}{4} + \frac{1}{48}.$$

If $\Delta < \frac{1}{2}$, the second case gives a smaller objective function value. Thus, k-means must fail to recover the two clusters if $\Delta < \frac{1}{2}$ and n is large.

However, the SDP relaxation of spectral clustering will not have this issue as demonstrated by the following theorem:

Theorem 4.2. *Let the data $\{x_i\}_{i=1}^{2n}$ be given by $\{x_{1,i}\}_{i=1}^n \cup \{x_{2,i}\}_{i=1}^n$ as defined in (4.3). Let Φ be the heat kernel with bandwidth*

$$\sigma^2 = \frac{\gamma}{(n-1)^2 \log(\frac{n}{\pi})}, \quad \gamma > 0.$$

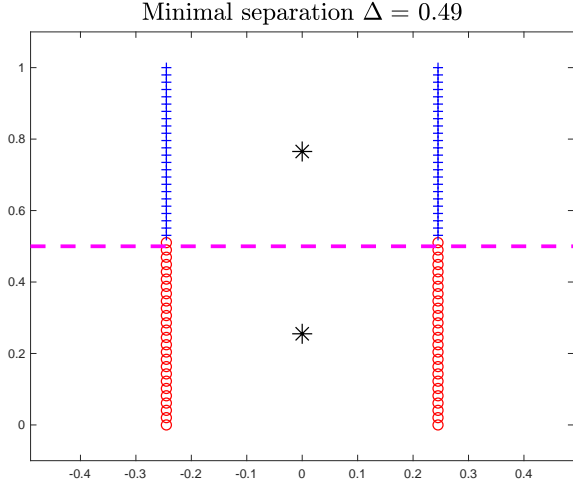
Assume the separation Δ satisfies

$$\Delta \geq \frac{1}{n-1} \sqrt{1 + \frac{6\gamma \log n}{\log(\frac{n}{\pi})}}.$$

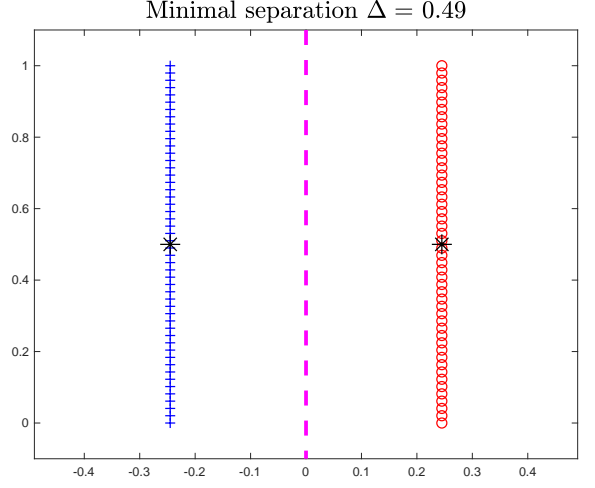
Then Algorithm 3 recovers the underlying two clusters $\{x_{1,i}\}_{i=1}^n$ and $\{x_{2,i}\}_{i=1}^n$ exactly.

The separation distance in Theorem 4.2 is nearly optimal, since the distance between adjacent points within a cluster is about $\frac{1}{n}$ and the distance between the clusters for which Algorithm 3 is guaranteed to return the correct clustering is $\Delta = \tilde{O}(\frac{1}{n})$.

²It is clear that in the given example simple rescaling of the data would make them more isotropic, but this is not the point we try to illustrate. Also, in more involved examples consisting of anisotropic clusters of different orientation, rescaling or resorting e.g. to the Mahalanobis distance instead of the Euclidean distance will not really overcome the sensibility of k-means to “geometric distortions”.



(a) The centroids are placed at $c_1 \approx [0 \ \frac{1}{4}]^\top$ and $c_2 \approx [0 \ \frac{3}{4}]^\top$.



(b) The centroids are placed at $c_1 = [-\frac{\Delta}{2} \ \frac{1}{2}]^\top$ and $c_2 = [\frac{\Delta}{2} \ \frac{1}{2}]^\top$.

Figure 2: The lines are separated by $\Delta = 0.49$ and 50 points are equi-spaced on the unit interval. The objective function values of the two scenarios above are approximately 8.1787 and 8.6735 for (a) and (b) respectively. In this case, the centroids in the left plot gives smaller k-means objective function value. Hence k-means criterion is unable to disentangle the two linearly separable manifolds if the two clusters are not well separated.

4.3 Examples with random data and open problems

From a practical viewpoint it is more appealing to consider random data instead of deterministic examples discussed above. However, in general, it is not an easy task to control the lower bound of the graph Laplacian from random data that are sampled from a probability density function supported on a manifold. Several factors will influence the spectrum of the graph Laplacian, e.g., the number of data points, the geometry of the manifold (shape, volume, connectivity, dimension, etc), the properties of probability density function, and the choice of kernel function $\Phi(\cdot)$ (w.l.o.g. we assume Φ is normalized, i.e., $\int \Phi(z) dz = 1$.) and its parameters, such as the bandwidth σ . We propose the following open problem and point out one possible solution.

Open Problem 4.3. *Suppose there are n data points drawn from a probability density function $p(x)$ supported on a manifold \mathcal{M} . How can we estimate the second smallest eigenvalue of the graph Laplacian (either normalized or unnormalized) given the kernel function Φ and σ ?*

In fact, numerous connections exist between graph Laplacians and Laplace-Beltrami operators on the manifold [43, 44, 40, 39, 12, 17]. Let L be the graph Laplacian constructed from $\{x_i\}_{i=1}^n$ sampled from a probability density function $p(x)$ supported on a Riemannian manifold \mathcal{M} with/without boundary. Define the weighted Laplace-Beltrami operator $\Delta_{\mathcal{M}}$ on \mathcal{M} as

$$\Delta_{\mathcal{M}}(f) := -\frac{1}{p} \text{div}(p^2 \nabla f)$$

where the divergence operator “div” and gradient “ ∇ ” are defined according to the Riemannian metric, cf [22]. The pointwise convergence of the graph Laplacian L to $\Delta_{\mathcal{M}}$ as well as the convergence of the normalized graph Laplacian have been discussed in several excellent works such as [12, 39, 18].

From our discussion in Section 3, one may have realized that the more relevant convergence of the graph Laplacian is spectral convergence: the convergence of the spectra of the graph Laplacian to those of its continuous limit and more importantly, *the convergence rate*. We make it more precise here: for the differential operator $\Delta_{\mathcal{M}}$, one considers the eigenvalue/eigenfunction problem with Neumann boundary condition:

$$\Delta_{\mathcal{M}} f = \lambda f \quad \text{in } \mathcal{M}, \quad \frac{\partial f}{\partial \mathbf{n}} = 0 \quad \text{on } \partial \mathcal{M} \quad (4.4)$$

where \mathbf{n} is the normal vector and $\partial\mathcal{M}$ is the boundary of \mathcal{M} . In particular, this problem reduces to an eigenvalue/eigenfunction problem if the manifold has no boundary.

We let $\lambda_2(\Delta_{\mathcal{M}})$ be the second smallest eigenvalue to (4.4). It has been shown in [44] that if \mathcal{M} is an open, bounded, and connected domain in \mathbb{R}^m with $m \geq 2$ and $\sigma = \tilde{\mathcal{O}}\left(\left(\frac{\log n}{n}\right)^{\frac{1}{2m}}\right)$, the rescaled second smallest eigenvalue $\frac{2}{n\sigma^2}\lambda_2(L)$ will converge to $\epsilon_{\Phi}\lambda_2(\Delta_{\mathcal{M}})$ almost surely when n gets larger where ϵ_{Φ} represents the surface tension³. Similar results also hold for the normalized graph Laplacian as shown in [44]. Moreover, [40] has extended the spectral convergence from graph Laplacians to connection Laplacians.

If one knows $\lambda_2(\Delta_{\mathcal{M}})$ for certain simple but important cases such as a line segment or a circle equipped with uniform distribution $p(x)$, it is possible to get an estimate of $\lambda_2(L)$ via $\lambda_2(\Delta_{\mathcal{M}})$ and obtain the performance guarantee of spectral clustering SDP from Theorems 3.1 and 3.2. A rigorous justification of this connection relies on the spectral convergence rate of the graph Laplacian to the Laplacian eigenvalue problem with Neumann boundary condition, which is still missing, to the best of our knowledge. Under proper conditions, [43] gives the spectral convergence rate of $\mathcal{O}\left(\left(\frac{\log n}{n}\right)^{\frac{1}{2m}}\right)$ for the graph Laplacian to converge to the Laplace-Beltrami operator on a Riemannian manifold \mathcal{M} . However, the kernel function Φ has a compact support which the heat kernel does not satisfy, and more severely, the manifold there is assumed to have no boundary. Thus we give another open problem, the solution of which will lead to a better and more complete understanding of SDP relaxation of spectral clustering for random data.

Open Problem 4.4. *Assume n data points are sampled independently from a probability density function $p(x)$ supported on \mathcal{M} and construct a graph Laplacian L with kernel function $\Phi(\cdot)$ with the size of neighborhood σ . What is the spectral convergence rate of the graph Laplacian to the Laplacian eigenvalue problem with Neumann boundary condition in (4.4)?*

4.4 Stochastic block model

The stochastic block model has been studied extensively as an example of community detection problem in the recent few years [2, 9, 1, 3, 4, 51]. Here we treat community detection problem under the stochastic block model as a special case of graph cuts problem. Let us quickly review the basics of stochastic block model. Assume there are two communities and each of them has n members and in total $N = 2n$ members. The adjacency matrix is a binary random matrix whose entries are given as follows,

1. if member i and j are in the same community, $\mathbb{P}(w_{ij} = 1) = p$ and $\mathbb{P}(w_{ij} = 0) = 1 - p$;
2. if member i and j are in different communities, $\mathbb{P}(w_{ij} = 1) = q$ and $\mathbb{P}(w_{ij} = 0) = 1 - q$.

Here $w_{ij} = w_{ji}$ and each w_{ij} is independent. We assume $p > q$ so that the connectivity within each individual community is stronger than that between different communities. The core question regarding the stochastic block model is to study when we are able to recover the underlying community exactly. Remarkable progress have been made by analyzing different types of convex relaxation and many performance bounds have been obtained so far. Interested readers may refer to the literature mentioned above for more details. Here we provide our performance bound in terms of p and q as an application of our theory to the stochastic block model.

Theorem 4.5. *Let $p = \frac{\alpha \log N}{N}$ and $q = \frac{\beta \log N}{N}$. The RatioCut-SDP (3.1) recovers the underlying communities exactly if*

$$\alpha > 40 \left(\frac{1}{3} + \frac{\beta}{2} + \sqrt{\frac{1}{9} + \beta} \right)$$

with high probability.

³Surface tension is defined as $\epsilon_{\Phi} = \int_{\mathbb{R}^m} |z^{(1)}|^2 \Phi(z) dz$ where $z^{(1)}$ is the first component of z .

We defer the proof of this theorem to Section 6.3. Compared with the state-of-the-art results such as [2, 9] where $\sqrt{\alpha} - \sqrt{\beta} > \sqrt{2}$ is needed for exact recovery, our performance bound is slightly looser by a constant factor. The near-optimal performance guarantee given by our analysis is not entirely surprising. As pointed out in [9], the Goemans-Williamson type of SDP relaxation⁴ succeeds if

$$\lambda_2(D_{\text{iso}} - D_\delta - W + \frac{1}{2}1_N 1_N^\top) > 0.$$

In fact, the condition above is implied by

$$\min \lambda_2(L_{\text{iso}}^{(a,a)}) > 2\|D_\delta\| \quad (4.5)$$

which differs from our Theorem 3.1 only by a constant factor. We leave the proof of this claim (4.5) in Section 6.3.

5 Numerical explorations

In this section, we present a few examples to complement our theoretic analysis. One key ingredient in Theorem 3.1 is the estimation of the second smallest eigenvalue of the graph Laplacian of each individual cluster. In general, it is not easy to estimate this quantity, especially for random instances. Therefore, we turn to certain numerical simulations to see if the *spectral proximity condition* holds for the data drawn from an underlying distribution supported on a manifold. We are in particular interested in the performances under different choices of minimal separation Δ and bandwidth σ . In general, the larger σ gets, the stronger the within and inter-cluster connectivity are. Thus σ cannot be arbitrarily large (just think about the extreme case $\sigma = \infty$ and the whole graph turns into a complete graph with equal edge weight); on the other hand, it is easier to pick a proper σ if the minimal separation Δ is larger. The rule of thumb of choosing σ is to increase the within-cluster connectivity while controlling the inter-cluster connectivity. We will also compare those numerical results with ordinary k-means (or k-means SDP) and demonstrate the advantage of spectral clustering.

5.1 Two parallel lines

In Section 4, we discuss two deterministic examples in which k-means fails to recover the underlying partition, as well as the conditions under which (3.1) and (3.2) succeed. Here we run numerical examples for their corresponding random instances and see how (3.5) and (3.6) work for RatioCut-SDP and NCut-SDP relaxation respectively.

In the first example, we assume the data are uniformly distributed on two concentric circles with radii $r_1 = 1$ and $r_2 = 1 + \Delta$. We sample $n = 250$ and $m = \lfloor 250(1 + \Delta) \rfloor$ for these two circles respectively so that the distance between two adjacent points on each circle is approximately $\mathcal{O}(\frac{1}{n})$. For each pair of (Δ, σ) , we run 50 experiments to see how many times the condition (3.5) and (3.6) hold respectively. More precisely, in the RatioCut-SDP, we compute the second smallest eigenvalue of Laplacian for each individual circle and $\|D_\delta\|$, and we treat the recovery is successful if (3.5) satisfies. Similar procedures are performed for NCut-SDP and count how many instances satisfy (3.6).

The size of the neighborhood σ is chosen as $\sigma = \frac{p}{n}$ with the horizontal parameter p in Figure 3 varying from 1 to 25; we test different values for the minimal separation Δ between two circles. The results are illustrated in Figure 3: the performances of RatioCut-SDP and NCut-SDP are quite similar. If $\Delta \geq 0.2$ and $5 \leq p \leq 75\Delta - 8$, then exact recovery is guaranteed with high probability. The distance between two adjacent points on one circle is approximately $\frac{2\pi}{n} \approx 0.025$ and our theorem succeeds if the minimal separation Δ is about 8 times larger than the “average” distance between adjacent points within one cluster.

⁴Here the Goemans-Williamson type of SDP relaxation is referred to $\max \text{Tr}((2W - (1_N 1_N^\top - I_N))Z)$, s.t. $Z \succeq 0$ and $Z_{ii} = 1$. Note this relaxation is designed specifically for the case of two clusters.

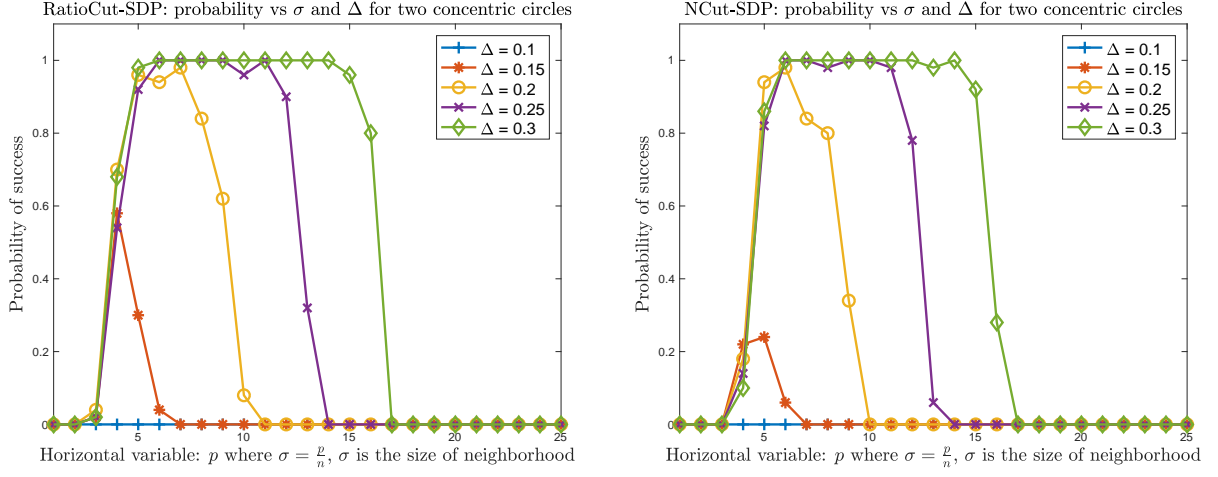


Figure 3: Two concentric circles with radii $r_1 = 1$ and $r_2 = 1 + \Delta$. The smaller circle has $n = 250$ uniformly distributed points and the larger one has $m = \lfloor 250(1 + \Delta) \rfloor$ where $\Delta = r_2 - r_1$. Left: RatioCut-SDP; Right: NCut-SDP.

5.2 Two concentric circles

For the two-lines case, we set two clusters as $[-\frac{\Delta}{2} x_i]^\top$ and $[\frac{\Delta}{2} y_i]^\top$, $1 \leq i \leq 250$ where all $\{x_i\}_{i=1}^n$ and $\{y_i\}_{i=1}^n$ are i.i.d. uniform random variables on $[0, 1]$. Thus the two clusters are exactly Δ apart. We also run 50 experiments for any pair of (Δ, σ) where $\sigma = \frac{p}{2n}$ with $1 \leq p \leq 20$ and $n = 250$. Then we compute how many of those random instances satisfy (3.5) and (3.6), similar to what we have done previously. Empirically, the SDP relaxation of spectral clustering achieves exact recovery with high probability if $\Delta \geq 0.05$ and $2 \leq p \leq 150\Delta - 4$, which outperforms the ordinary k-means by a huge margin. Recall that in k-means, when $\Delta < \frac{1}{2}$ and n is large, the global minimum of k-means is unable to detect the underlying clusters correctly. Here, the SDP relaxation works provably even if $\Delta \geq 0.05$ which is very close to $\frac{\log n}{n}$ where $n = 250$.

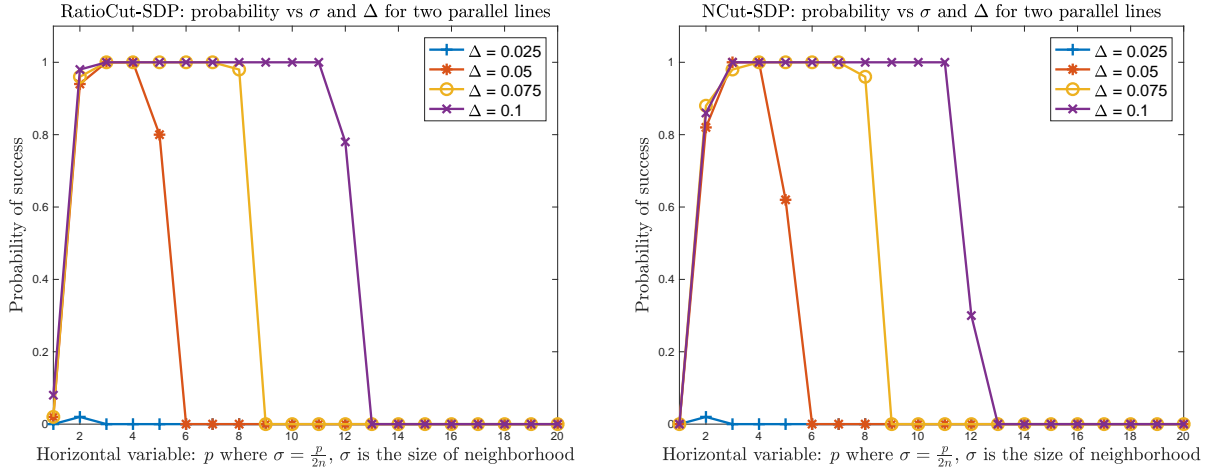


Figure 4: Two parallel line segments of unit length with separation Δ and 250 points are sampled uniformly on each line. Left: RatioCut-SDP; Right: NCut-SDP.

5.3 Stochastic ball model and comparison with k-means

Now we apply Theorems 3.1 and 3.2 to the stochastic ball model with two clusters located on a 2D plane and compare the results with those via k-means SDP. The stochastic ball model is believed in a way optimal for k-means: the clusters are within convex boundaries and perfectly isotropic. However, we will find spectral clustering SDP performs much better. Consider the

stochastic ball model with two clusters which satisfy

$$x_{1,i} = \begin{bmatrix} -\frac{\Delta}{2} - 1 \\ 0 \end{bmatrix} + r_{1,i}, \quad x_{2,i} = \begin{bmatrix} \frac{\Delta}{2} + 1 \\ 0 \end{bmatrix} + r_{2,i}$$

where $\{r_{1,i}\}_{i=1}^n$ and $\{r_{2,i}\}_{i=1}^n$ are i.i.d. uniform random vectors on the 2D unit disk. From the definition, we know that the support of probability density function of each cluster is included in a unit disk centered at $[-\frac{\Delta}{2} - 1 \ 0]^\top$ and $[\frac{\Delta}{2} + 1 \ 0]^\top$ respectively. If $\Delta > 0$, then the supports of those two distributions are separated by at least Δ .

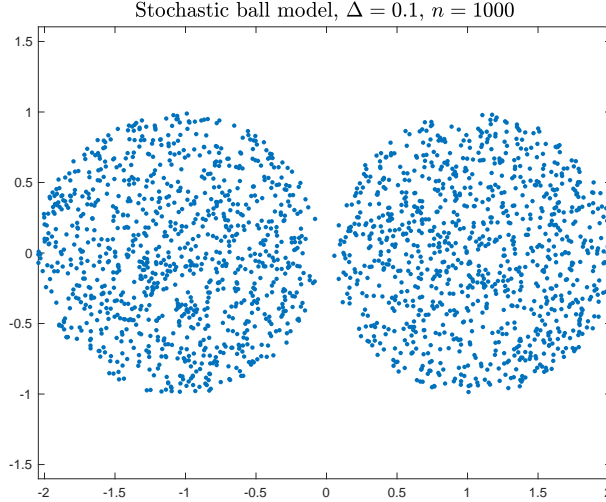


Figure 5: Stochastic ball model with two clusters and the separation between the centers is $2 + \Delta$. Each cluster has 1000 points.

The results are illustrated in Figure 6 and 7, and we summarize the empirical sufficient condition for exact recovery in terms of n , σ , and Δ :

1. if $n = 250$, we require $\Delta \geq 0.2$, $\sigma = \frac{p}{5\sqrt{n}}$ and $2 \leq p \leq 40\Delta - 4$;
2. if $n = 1000$, we require $\Delta \geq 0.1$, $\sigma = \frac{p}{5\sqrt{n}}$, and $2 \leq p \leq 60\Delta - 2$.

In other words, when the number of points increases, the minimal separation Δ for exact recovery will also decrease because a smaller σ can be picked to ensure strong within-cluster connectivity while the inter-cluster connectivity diminishes simultaneously for a fixed Δ .

To compare the performance of spectral clustering SDP with that of k-means SDP, we use a necessary condition in [32]. The k-means SDP is exactly in the form of (3.1) but the graph Laplacian L is replaced by squared distance matrix of data. The necessary condition in [32] states that the exact recovery via k-means SDP is impossible if

$$\Delta \leq \sqrt{\frac{3}{2}} - 1 \approx 0.2247.$$

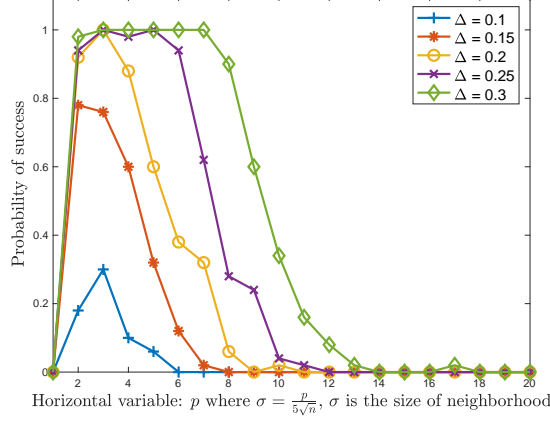
On the other hand, we see much better performance via (3.1) and (3.2) from Figure 6 and 7 respectively. Even if the separation Δ is below 0.2, one can still achieve exact recovery with high probability with a proper choice of $\sigma = \mathcal{O}(\frac{1}{\sqrt{n}})$.

6 Proofs

6.1 Proofs of Theorem 3.1 and 3.2

To certify X in (3.3) as the global minimizer of (3.1) and (3.2), we resort to the powerful tool of Lagrangian duality theory [15, 13]. While some of the calculations follow from our previous paper [32], we include them to make the presentation more self-contained. The proof starts

RatioCut-SDP: probability vs σ and Δ for stochastic ball model, $n = 250$



RatioCut-SDP: probability vs σ and Δ for stochastic ball model, $n = 1000$

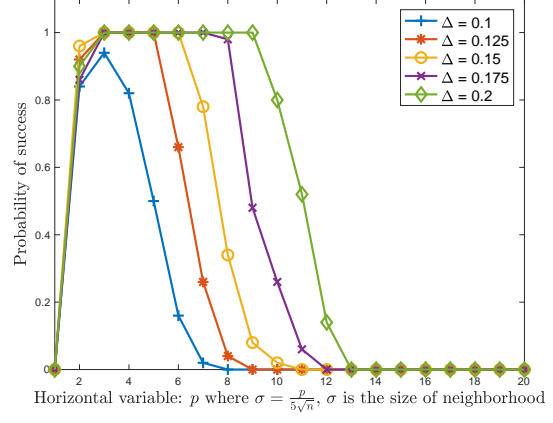
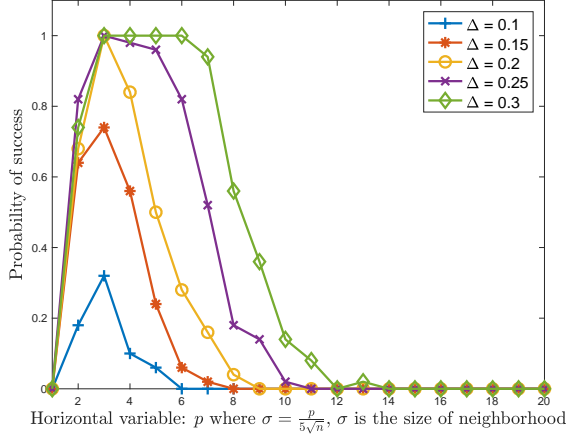


Figure 6: Performance of RatioCut-SDP for 2D stochastic ball model. Left: each ball has $n = 250$ points; Right: each ball contains $n = 1000$ points.

NCut-SDP: probability vs σ and Δ for stochastic ball model, $n = 250$



NCut-SDP: probability vs σ and Δ for stochastic ball model, $n = 1000$

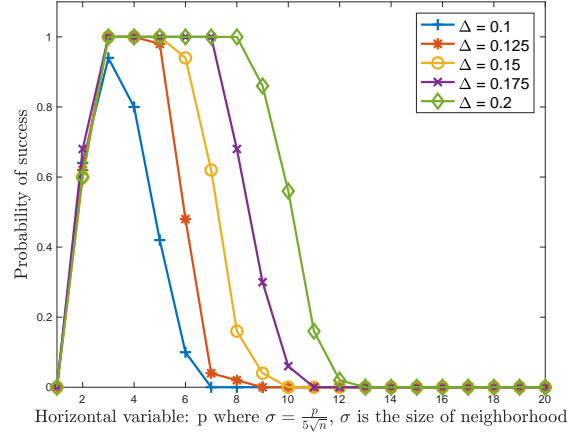


Figure 7: Performance of NCut-SDP for 2D stochastic ball model. Left: each ball has $n = 250$ points; Right: each ball contains $n = 1000$ points.

with finding a sufficient condition that guarantees X to be the global minimizer and then we show the assumptions in Theorem 3.1 and 3.2 satisfy the proposed sufficient conditions.

In our proof, we will use the famous Gershgorin circle theorem repeatedly, the proof of which can be found in many sources such as [23, Chapter 7].

Theorem 6.1 (Gershgorin circle theorem). *Given a matrix $Z = (z_{ij})_{1 \leq i, j \leq n} \in \mathbb{R}^{n \times n}$ and all of its eigenvalues $\{\lambda_l(Z)\}_{l=1}^n$ are contained in the union of the circles centered at $\{z_{ii}\}_{i=1}^n$,*

$$\{\lambda_l(Z)\}_{l=1}^n \subseteq \bigcup_{i=1}^n \left\{ x \in \mathbb{C} \mid |x - z_{ii}| \leq \sum_{j \neq i} |z_{ij}| \right\}.$$

In particular, if Z is also nonnegative, all the eigenvalues satisfy

$$\max_{1 \leq l \leq n} |\lambda_l(Z)| \leq \|Z\|_{\infty}.$$

6.1.1 Notation and preliminaries

To begin with, we introduce a few notations. Due to the similarity between the programs (3.1) and (3.2), we combine them into the following general form:

$$\min_{Z \in \mathcal{S}_N} \langle A, Z \rangle, \quad \text{s.t.} \quad Z \succeq 0, \quad Z \geq 0, \quad \text{Tr}(Z) = k, \quad Z\varphi = \varphi. \quad (6.1)$$

Here $\varphi \in \mathbb{R}^N$, $\varphi_a \in \mathbb{R}^{n_a}$ (which is the a -th block of φ), and A are defined as follows:

1. For RatioCut-SDP in (3.1),

$$\varphi := 1_N, \quad \varphi_a := 1_{n_a}, \quad A := L, \quad \tau = \frac{\max_l n_l}{\min_l n_l}. \quad (6.2)$$

2. For NCut-SDP in (3.2),

$$\varphi := D^{\frac{1}{2}} 1_N, \quad \varphi_a := (D^{(a,a)})^{\frac{1}{2}} 1_{n_a}, \quad A := L_{\text{sym}}, \quad \tau = \frac{\max_l \text{vol}(\Gamma_l)}{\min_l \text{vol}(\Gamma_l)}. \quad (6.3)$$

With the definition of φ_a in (6.2) and (6.3), we can put the ground truth X into a unifying form

$$X^{(a,a)} = \frac{1}{\|\varphi_a\|^2} \varphi_a \varphi_a^\top, \quad X^{(a,b)} = 0, \quad a \neq b$$

which is a block-diagonal matrix.

Our theoretic analysis also rely on a few commonly used convex cones. Let \mathcal{K} and \mathcal{K}^* be a pair of cone and dual cone⁵:

$$\mathcal{K} = \mathcal{S}_N^+ \cap \mathbb{R}_+^{N \times N}, \quad \mathcal{K}^* = \mathcal{S}_N^+ + \mathbb{R}_+^{N \times N} = \{Q + B : Q \succeq 0, B \geq 0\} \quad (6.4)$$

where \mathcal{K} is the intersection of two self-dual cones, i.e., the positive semi-definite cone \mathcal{S}_N^+ and the nonnegative cone $\mathbb{R}_+^{N \times N}$. By definition, \mathcal{K} is a pointed⁶ and closed convex cone with a nonempty interior. For the last two constraints in (6.1), we define a useful linear operator \mathcal{A} which maps \mathcal{S}_N to \mathbb{R}^{N+1} as follows

$$\mathcal{A} : \mathcal{S}_N \rightarrow \mathbb{R}^{N+1} : \quad \mathcal{A}(Z) = \begin{bmatrix} \langle I_N, Z \rangle \\ \frac{1}{2}(Z + Z^\top)\varphi \end{bmatrix}. \quad (6.5)$$

Obviously, there hold $\text{Tr}(Z) = \langle I_N, Z \rangle$ and $Z\varphi = \frac{1}{2}(Z + Z^\top)\varphi$, and thus the last two constraints in (6.1) can be written as

$$\mathcal{A}(X) = \begin{bmatrix} k \\ \varphi \end{bmatrix} =: b.$$

Its dual operator \mathcal{A}^* under the canonical inner product over $\mathbb{R}^{N \times N}$ is given by

$$\mathcal{A}^*(\lambda) := \frac{1}{2}(\alpha\varphi^\top + \varphi\alpha^\top) + zI_N$$

where $\lambda := \begin{bmatrix} z \\ \alpha \end{bmatrix} \in \mathbb{R}^{N+1}$ is the dual variable with $z \in \mathbb{R}$ and $\alpha \in \mathbb{R}^N$. Therefore, an equivalent form of (6.1) is

$$\min_{Z \in \mathcal{K}} \langle A, Z \rangle, \quad \text{s.t.} \quad \mathcal{A}(Z) = b.$$

The Lagrangian function can be expressed in the form of

$$\mathcal{L}(Z, \lambda) := \langle A, Z \rangle + \langle \lambda, \mathcal{A}(Z) - b \rangle = \langle \mathcal{A}^*(\lambda) + A, Z \rangle - \langle \lambda, b \rangle.$$

By taking the infimum over $\mathcal{K} := \{Z : Z \succeq 0, Z \geq 0\}$, we have

$$\inf_{Z \in \mathcal{K}} \mathcal{L}(Z, \lambda) = -\langle \lambda, b \rangle$$

if $\mathcal{A}^*(\lambda) + A \in \mathcal{K}^*$ and then obtain the dual program of (6.1):

$$\max -\langle \lambda, b \rangle, \quad \text{s.t.} \quad \mathcal{A}^*(\lambda) + A \in \mathcal{K}^*.$$

Here $\mathcal{A}^*(\lambda) + A \in \mathcal{K}^*$ means it can be written as the sum of a positive semidefinite matrix and a nonnegative matrix, i.e.,

$$\mathcal{A}^*(\lambda) + A = Q + B, \quad (6.6)$$

⁵The dual cone \mathcal{K}^* of \mathcal{K} is defined as $\{W : \langle W, Z \rangle \geq 0, \forall Z \in \mathcal{K}\}$; in particular, there holds $(\mathcal{K}^*)^* = \mathcal{K}$.

⁶The cone \mathcal{K} is pointed if for $Z \in \mathcal{K}$ and $-Z \in \mathcal{K}$, Z must be 0, see Chapter 2 in [13].

where $Q \succeq 0$ and $B \geq 0$.

Finally, we define two linear subspaces on \mathcal{S}_N which will be useful later:

$$\begin{aligned} T &:= \{XZ + ZX - XZX : Z \in \mathcal{S}_N\}, \\ T^\perp &:= \{(I_N - X)Z(I_N - X) : Z \in \mathcal{S}_N\}. \end{aligned} \quad (6.7)$$

We then denote Z_T and Z_{T^\perp} as the orthogonal projection of Z onto T and T^\perp respectively.

6.1.2 Optimality condition and dual certificate

From the theory of convex optimization [13], we know that X is a global minimizer (not necessarily unique) of (6.1) if complementary slackness holds

$$\langle \mathcal{A}^*(\lambda) + A, X \rangle = \langle Q + B, X \rangle = 0$$

where λ is the dual variable. From complementary slackness, we are able to find a few useful relations regarding B, Q , and X .

From $Q \succeq 0$, $B \geq 0$, and $X \in \mathcal{K}$, we have

$$\langle Q, X \rangle = \langle B, X \rangle = 0$$

because both $\langle Q, X \rangle$ and $\langle B, X \rangle$ are nonnegative, and their sum equals 0. Moreover, there hold

$$B^{(a,a)} = 0, \quad QX = 0 \quad (6.8)$$

where $B^{(a,a)} = 0$ follows from $X^{(a,a)} = \frac{1}{\|\varphi_a\|^2} \varphi_a \varphi_a^\top > 0$ and

$$0 = \langle B, X \rangle = \sum_{a=1}^k \frac{1}{\|\varphi_a\|^2} \langle B^{(a,a)}, \varphi_a \varphi_a^\top \rangle.$$

On the other hand, $QX = 0$ follows from $\langle Q, X \rangle = 0$, $Q \succeq 0$, and $X \succeq 0$. By definition of T^\perp in (6.7), we can see that $QX = 0$ implies $Q \in T^\perp$.

With the discussion above, we are ready to present a sufficient condition to certify X as the unique global minimizer of (6.1).

Proposition 6.2 (Sufficient condition). *Suppose X is a feasible solution of (6.1) and there exists Q such that $Q \succeq 0$ and X satisfies $QX = 0$ where Q is defined in (6.6). Then X is the unique minimizer of (6.1) if $B^{(a,b)} > 0$ for all $a \neq b$ and $B^{(a,a)} = 0$.*

Note that the choices of Q and B are not arbitrary; the sum of Q and B must satisfy $Q + B = \mathcal{A}^*(\lambda) + A$ for certain λ .

Proof of Proposition 6.2. Let \tilde{X} be another feasible solution, i.e., $\tilde{X} \in \mathcal{K}$ and $\mathcal{A}(\tilde{X}) = b$ but $\tilde{X} \neq X$. The goal is to show that $\langle A, \tilde{X} \rangle > \langle A, X \rangle$, i.e., the objective function value evaluated at \tilde{X} is strictly larger than that evaluated at X .

Assume $\mathcal{A}^*(\lambda) + A = Q + B$ for certain λ . Since \tilde{X} and Q are positive semidefinite, we have $\langle \tilde{X}, Q \rangle \geq 0$. Hence, there holds

$$\begin{aligned} \langle Q, \tilde{X} \rangle &= \langle Q, \tilde{X} - X \rangle = \langle \mathcal{A}^*(\lambda) + A - B, \tilde{X} - X \rangle \\ &= \langle A - B, \tilde{X} - X \rangle \geq 0 \end{aligned}$$

which follows from $Q \succeq 0$, $QX = 0$, and both \tilde{X} and X satisfy the linear constraints. Therefore, combined with $\langle B, X \rangle = 0$, we get

$$\langle A, \tilde{X} \rangle - \langle A, X \rangle \geq \langle B, \tilde{X} - X \rangle = \langle B, \tilde{X} \rangle \geq 0.$$

Hence, it suffices to show that $\langle B, \tilde{X} \rangle > 0$ under $B^{(a,b)} > 0$. We achieve this by proving $\langle B, \tilde{X} \rangle = 0$ if and only if $\tilde{X} = X$.

Suppose $\langle B, \tilde{X} \rangle = 0$ and $B^{(a,b)} > 0$, then $\tilde{X}^{(a,b)} = 0$ follows from

$$\sum_{a=1}^k \sum_{b=1}^k \langle B^{(a,b)}, \tilde{X}^{(a,b)} \rangle = 0 \iff \langle B^{(a,b)}, \tilde{X}^{(a,b)} \rangle = 0.$$

In other words, the support of \tilde{X} is contained in that of X , i.e., \tilde{X} is also a block-diagonal matrix. Therefore, combined with $\tilde{X}\varphi = \varphi$, we have $\tilde{X}^{(a,a)}\varphi_a = \varphi_a$ which means \tilde{X} has 1 as an eigenvalue with multiplicity k . On the other hand, $\text{Tr}(\tilde{X}) = k$ along with $\tilde{X} \succeq 0$ implies that each block of \tilde{X} is rank-1 and must satisfy $\tilde{X} = X$. \square

According to Proposition 6.2, it suffices to construct B and Q such that $QX = 0$, $Q \succeq 0$, $B^{(a,a)} = 0$, and $B^{(a,b)} > 0$ for all $a \neq b$. Note that

$$Q = \frac{1}{2}(\alpha\varphi^\top + \varphi\alpha^\top) + zI_N + A - B \quad (6.9)$$

which contains three unknowns α , z , and B . In fact, we are able to determine α in terms of z and hence by the following lemma, we express Q explicitly in terms of z and B which can be found in (6.13) and (6.14). This is made possible by $QX = 0$ which is equivalent to

$$Q^{(a,b)}\varphi_b = 0, \quad \forall a, b. \quad (6.10)$$

Lemma 6.3. *Given $QX = 0$ and $Q \succeq 0$, the a -th block of $\alpha \in \mathbb{R}^N$ is determined by*

$$\alpha_a = -\frac{2}{\|\varphi_a\|^2}A^{(a,a)}\varphi_a - \frac{1}{\|\varphi_a\|^2} \left(z - \frac{\varphi_a^\top A^{(a,a)}\varphi_a}{\|\varphi_a\|^2} \right) \varphi_a. \quad (6.11)$$

Proof: By definition of $Q^{(a,a)}$ in (6.9) and $B^{(a,a)} = 0$, we have

$$Q^{(a,a)}\varphi_a = \left(\frac{1}{2}(\alpha_a\varphi_a^\top + \varphi_a\alpha_a^\top) + zI_{n_a} + A^{(a,a)} \right) \varphi_a = 0.$$

Solving for α_a gives

$$\alpha_a = -\frac{2}{\|\varphi_a\|^2}A^{(a,a)}\varphi_a - \frac{1}{\|\varphi_a\|^2}(\alpha_a^\top\varphi_a + 2z)\varphi_a. \quad (6.12)$$

Multiplying both sides with φ_a^\top from the left gives an expression of $\alpha_a^\top\varphi_a$, i.e.,

$$\alpha_a^\top\varphi_a = -\frac{2}{\|\varphi_a\|^2}\varphi_a^\top A^{(a,a)}\varphi_a - (\alpha_a^\top\varphi_a + 2z) \implies \alpha_a^\top\varphi_a = -\frac{1}{\|\varphi_a\|^2}\varphi_a^\top A^{(a,a)}\varphi_a - z$$

Plugging $\alpha_a^\top\varphi_a$ back to (6.12) finishes the proof. \square

Once we have α_a in (6.11) and substitute it into (6.9), we have an explicit expression for $Q^{(a,b)}$:

$$\begin{aligned} Q^{(a,b)} &= -\left(\frac{A^{(a,a)}\varphi_a\varphi_b^\top}{\|\varphi_a\|^2} + \frac{\varphi_a\varphi_b^\top A^{(b,b)}}{\|\varphi_b\|^2} \right) + \frac{1}{2} \left(\frac{\varphi_a^\top A^{(a,a)}\varphi_a}{\|\varphi_a\|^4} + \frac{\varphi_b^\top A^{(b,b)}\varphi_b}{\|\varphi_b\|^4} \right) \varphi_a\varphi_b^\top \\ &\quad - \frac{z}{2} \left(\frac{1}{\|\varphi_a\|^2} + \frac{1}{\|\varphi_b\|^2} \right) \varphi_a\varphi_b^\top + (A^{(a,b)} - B^{(a,b)}). \end{aligned} \quad (6.13)$$

For diagonal blocks $Q^{(a,a)}$,

$$\begin{aligned} Q^{(a,a)} &= \frac{1}{2}(\alpha_a\varphi_a^\top + \varphi_a\alpha_a^\top) + zI_{n_a} + A^{(a,a)} \\ &= -\frac{A^{(a,a)}\varphi_a\varphi_a^\top + \varphi_a\varphi_a^\top A^{(a,a)}}{\|\varphi_a\|^2} + z \left(I_{n_a} - \frac{\varphi_a\varphi_a^\top}{\|\varphi_a\|^2} \right) + \frac{\varphi_a^\top A^{(a,a)}\varphi_a}{\|\varphi_a\|^4} \varphi_a\varphi_a^\top + A^{(a,a)} \\ &= \left(I_{n_a} - \frac{\varphi_a\varphi_a^\top}{\|\varphi_a\|^2} \right) (A^{(a,a)} + zI_{n_a}) \left(I_{n_a} - \frac{\varphi_a\varphi_a^\top}{\|\varphi_a\|^2} \right). \end{aligned} \quad (6.14)$$

Now we summarize the discussion and clarify our goal: we want to pick up z and B such that

1. $Q^{(a,b)}\varphi_b = 0$ which is equivalent to $QX = 0$. Moreover, with direct computation, one can show that $B^{(a,b)}$ must satisfy

$$B^{(a,b)}\varphi_b = \|\varphi_b\|^2 u_{a,b} \in \mathbb{R}^{n_a} \quad (6.15)$$

where $u_{a,b}$ only depends on z and satisfies

$$\begin{aligned} u_{a,b} := & \frac{A^{(a,b)}\varphi_b}{\|\varphi_b\|^2} - \frac{A^{(a,a)}\varphi_a}{\|\varphi_a\|^2} + \frac{1}{2} \left(\frac{\varphi_a^\top A^{(a,a)}\varphi_a}{\|\varphi_a\|^4} - \frac{\varphi_b^\top A^{(b,b)}\varphi_b}{\|\varphi_b\|^4} \right) \varphi_a \\ & - \frac{z}{2} \left(\frac{1}{\|\varphi_a\|^2} + \frac{1}{\|\varphi_b\|^2} \right) \varphi_a. \end{aligned} \quad (6.16)$$

2. Q is positive semidefinite, i.e., $Q \succeq 0$. In fact, we have $Q \in T^\perp$ since $QX = 0$.

3. $B^{(a,b)} > 0$, $B^{(a,a)} = 0$, and B is symmetric.

Finally, we arrive at the following requirements for the constructions of dual certificate:

$$B^{(a,b)}\varphi_b = \|\varphi_b\|^2 u_{a,b}, \quad Q_{T^\perp} \succeq 0, \quad B^{(a,b)} > 0, \quad B^{(a,a)} = 0 \quad (6.17)$$

for all $a \neq b$ where $u_{a,b}$ depends on z in (6.16).

Here we simply choose B as

$$B^{(a,b)} = \frac{\|\varphi_b\|^2}{u_{b,a}^\top \varphi_b} u_{a,b} u_{b,a}^\top. \quad (6.18)$$

Lemma 6.4 implies the B in (6.18) satisfies (6.15) and moreover B is symmetric. With (6.18), there is *only one* variable z to be determined since B is now a function of z , as implied by (6.18) and (6.15). Next, we will prove that a choice of z exists such that $B \geq 0$ and $Q_{T^\perp} \succeq 0$ hold simultaneously under the assumptions in Theorem 3.1 and 3.2. Combining all those results together finishes our proof.

Lemma 6.4. *The matrix B is symmetric and satisfies (6.15) under the construction of B in (6.18).*

Proof of Lemma 6.4. By construction of $B^{(a,b)}$ in (6.18), we have

$$B^{(a,b)}\varphi_b = \|\varphi_b\|^2 u_{a,b}$$

which satisfies (6.15). To show that $B^{(a,b)} = (B^{(b,a)})^\top$, it suffices to show

$$\frac{u_{b,a}^\top \varphi_b}{\|\varphi_b\|^2} = \frac{u_{a,b}^\top \varphi_a}{\|\varphi_a\|^2}, \quad \forall a \neq b. \quad (6.19)$$

Direct computations gives

$$u_{a,b}^\top \varphi_a = \frac{\varphi_a^\top A^{(a,b)}\varphi_b}{\|\varphi_b\|^2} - \frac{\|\varphi_a\|^2}{2} \left(\frac{\varphi_a^\top A^{(a,a)}\varphi_a}{\|\varphi_a\|^4} + \frac{\varphi_b^\top A^{(b,b)}\varphi_b}{\|\varphi_b\|^4} \right) - \frac{\|\varphi_a\|^2 z}{2} \left(\frac{1}{\|\varphi_a\|^2} + \frac{1}{\|\varphi_b\|^2} \right).$$

Note that $\frac{u_{b,a}^\top \varphi_b}{\|\varphi_b\|^2}$ and $\frac{u_{a,b}^\top \varphi_a}{\|\varphi_a\|^2}$ have the same terms except their first terms $\varphi_a^\top A^{(a,b)}\varphi_b$ and $\varphi_b^\top A^{(b,a)}\varphi_a$. By definition of φ_a and $A^{(a,b)}$ in (6.2) and (6.3), we have

$$\varphi_a^\top A^{(a,b)}\varphi_b = \begin{cases} 1_{n_a}^\top L^{(a,b)} 1_{n_b}, & \text{if } A = L, \\ 1_{n_a}^\top (D^{(a,a)})^{\frac{1}{2}} L_{\text{sym}}^{(a,b)} (D^{(b,b)})^{\frac{1}{2}} 1_{n_b} = 1_{n_a}^\top L^{(a,b)} 1_{n_b}, & \text{if } A = L_{\text{sym}}, \end{cases}$$

where $L_{\text{sym}}^{(a,b)} = (D^{(a,a)})^{-\frac{1}{2}} L^{(a,b)} (D^{(b,b)})^{-\frac{1}{2}}$. Since $L^{(a,b)} = -W^{(a,b)}$ and $W^{(a,b)} = (W^{(b,a)})^\top$, there holds

$$\varphi_a^\top A^{(a,b)}\varphi_b = \varphi_b^\top A^{(b,a)}\varphi_a, \quad a \neq b.$$

Then we have (6.19) and B is symmetric. □

6.1.3 Proof of Theorem 3.1

Proposition 6.5 (Proof of Theorem 3.1). *Assume we have*

$$\|D_\delta\| \leq \frac{\min_{1 \leq a \leq k} \lambda_2(L_{\text{iso}}^{(a,a)})}{2(k-1)(\tau+1)+3}$$

and B is chosen in (6.18). Let $z = -3\|D_\delta\|$ and then for all $a \neq b$,

$$B^{(a,b)} > 0, \quad Q_{T^\perp} \succeq 0, \quad (6.20)$$

hold simultaneously which certifies X_{rcut} as the unique global minimizer to (3.1).

Proof: In this RatioCut case, we set

$$\varphi_a = 1_{n_a}, \quad A = L, \quad \tau = \frac{\max_l n_l}{\min_l n_l}$$

according to (6.2) and (3.4). The proof proceeds in two steps: we first give a bound for z such that $B^{(a,b)} = \frac{n_b}{u_{b,a}^\top 1_{n_b}} u_{a,b} u_{b,a}^\top > 0$ hold and $Q_{T^\perp} \succeq 0$ respectively; then we show such a parameter z exists under the assumption of Theorem 3.1.

Step 1: A sufficient condition for $B^{(a,b)} > 0$. We claim that if $z \leq -3\|D_\delta\|$, then $B^{(a,b)} > 0$. By the construction of $B^{(a,b)}$, it suffices to ensure $u_{a,b} > 0$ for all $a \neq b$. Now we give lower bounds for each term in $u_{a,b}$:

$$u_{a,b} := \frac{L^{(a,b)} 1_{n_b}}{n_b} - \frac{L^{(a,a)} 1_{n_a}}{n_a} + \frac{1}{2} \left(\frac{1_{n_a}^\top L^{(a,a)} 1_{n_a}}{n_a^2} - \frac{1_{n_b}^\top L^{(b,b)} 1_{n_b}}{n_b^2} \right) 1_{n_a} - \frac{z}{2} \left(\frac{1}{n_a} + \frac{1}{n_b} \right) 1_{n_a}. \quad (6.21)$$

By definition of $L^{(a,b)}$, we have $L^{(a,b)} = -W^{(a,b)}$ and

$$L^{(a,a)} 1_{n_a} = - \sum_{l \neq a} L^{(a,l)} 1_{n_l} = \sum_{l \neq a} W^{(a,l)} 1_{n_l} \quad (6.22)$$

which follows from $L 1_N = 0$. Due to the nonnegativity of $W^{(a,b)}$, there holds

$$0 \leq L^{(a,a)} 1_{n_a} = \sum_{l \neq a} W^{(a,l)} 1_{n_l} \leq \|D_\delta\| 1_{n_a}. \quad (6.23)$$

Therefore, we get lower bounds for both $L^{(a,b)} 1_{n_b}$ and $-L^{(a,a)} 1_{n_a}$ as follows:

$$L^{(a,b)} 1_{n_b} = -W^{(a,b)} 1_{n_b} \geq -\|D_\delta\| 1_{n_a}, \quad -L^{(a,a)} 1_{n_a} = - \sum_{l \neq a} W^{(a,l)} 1_{n_l} \geq -\|D_\delta\| 1_{n_a}. \quad (6.24)$$

For $\frac{1_{n_a}^\top L^{(a,a)} 1_{n_a}}{n_a^2} - \frac{1_{n_b}^\top L^{(b,b)} 1_{n_b}}{n_b^2}$, we first apply (6.22)

$$\frac{1_{n_a}^\top L^{(a,a)} 1_{n_a}}{n_a^2} - \frac{1_{n_b}^\top L^{(b,b)} 1_{n_b}}{n_b^2} = \frac{1}{n_a^2} \sum_{l \neq a} 1_{n_a}^\top W^{(a,l)} 1_{n_l} - \frac{1}{n_b^2} \sum_{l \neq b} 1_{n_b}^\top W^{(b,l)} 1_{n_l}$$

and then (6.23) again implies

$$-\frac{1}{n_b} \|D_\delta\| 1_{n_a} \leq \left(\frac{1_{n_a}^\top L^{(a,a)} 1_{n_a}}{n_a^2} - \frac{1_{n_b}^\top L^{(b,b)} 1_{n_b}}{n_b^2} \right) 1_{n_a} \leq \frac{1}{n_a} \|D_\delta\| 1_{n_a}. \quad (6.25)$$

By combining (6.24) and (6.25) with (6.21), we obtain

$$\begin{aligned} \frac{1}{n_b} B^{(a,b)} 1_{n_b} = u_{a,b} &\geq - \left(\frac{1}{n_b} + \frac{1}{n_a} + \frac{1}{2n_b} \right) \|D_\delta\| 1_{n_a} - \frac{z}{2} \left(\frac{1}{n_a} + \frac{1}{n_b} \right) 1_{n_a} \\ &\geq - \left(\frac{1}{n_a} + \frac{3}{2n_b} \right) \|D_\delta\| 1_{n_a} + \frac{3}{2} \left(\frac{1}{n_a} + \frac{1}{n_b} \right) \|D_\delta\| 1_{n_a} > 0 \end{aligned}$$

where $z \leq -3\|D_\delta\|$.

Step 2: A sufficient condition for $Q_{T^\perp} \succeq 0$. The equations $B^{(a,b)}1_{n_b} = n_b u_{a,b} > 0$ guarantee $Q \in T^\perp$ and thus it suffices to show $Q_{T^\perp} \succeq 0$. We will show the claim is true if $z \geq \frac{(k-1)\tau\|D_\delta\| - 2\min_{1 \leq a \leq k} \lambda_2(L_{\text{iso}}^{(a,a)})}{(k-1)(\tau+1)+2}$. First we project Q to T^\perp and then each projected $Q^{(a,b)}$ obeys

$$\begin{aligned} Q_{T^\perp}^{(a,b)} &= \left(I_{n_a} - \frac{1}{n_a} J_{n_a \times n_a} \right) (L^{(a,b)} - B^{(a,b)}) \left(I_{n_b} - \frac{1}{n_b} J_{n_b \times n_b} \right), \quad a \neq b, \\ Q_{T^\perp}^{(a,a)} &= \left(I_{n_a} - \frac{J_{n_a \times n_a}}{n_a} \right) (L^{(a,a)} + z I_{n_a}) \left(I_{n_a} - \frac{J_{n_a \times n_a}}{n_a} \right), \quad a = b, \end{aligned}$$

which follow from the expression of $Q^{(a,b)}$ in (6.13) and (6.14).

Let $v \in \mathbb{R}^N$ be a unit vector in T^\perp and that means $Xv = 0 \in \mathbb{R}^k$, i.e., $1_{n_a}^\top v_a = 0$ for $1 \leq a \leq k$ where v_a is the a -th block of v . We aim to prove $v^\top Qv \geq 0$ for all such $v \in \mathbb{R}^N$ and $\|v\| = 1$. There hold

$$v^\top Qv = v^\top (L + zI_N - B)v = v^\top (L_{\text{iso}} + L_\delta) - v^\top Bv + z \geq \underbrace{\sum_{1 \leq a \leq k} v_a^\top L_{\text{iso}}^{(a,a)} v_a}_{\Pi_1} - \underbrace{v^\top Bv}_{\Pi_2} + z \quad (6.26)$$

where $L = L_{\text{iso}} + L_\delta$ is in (2.9) and $L_\delta = D_\delta - W_\delta \succeq 0$ since L_δ is a graph Laplacian.

For the first term, we have

$$\Pi_1 = \sum_{1 \leq a \leq k} v_a^\top L_{\text{iso}}^{(a,a)} v_a \geq \sum_{a=1}^k \lambda_2(L_{\text{iso}}^{(a,a)}) \|v_a\|^2 \geq \min_{1 \leq a \leq k} \lambda_2(L_{\text{iso}}^{(a,a)}) \quad (6.27)$$

where the second last inequality follows from $v_a^\top 1_{n_a} = 0$ and $L_{\text{iso}}^{(a,a)} 1_{n_a} = 0$, and the variational form for the second smallest eigenvalue of symmetric matrices.

For the second term Π_2 , we have $|\Pi_2| \leq \|B\|$. Now we try to estimate $\|B\|$ under the assumption $B \geq 0$ which is guaranteed by $z \leq -3\|D_\delta\|$ in Step 1. From (6.25), (6.24), and (6.21), we have

$$\begin{aligned} 0 &\leq \frac{1}{n_b} B^{(a,b)} 1_{n_b} = u_{a,b} \leq -\frac{W^{(a,b)} 1_{n_b}}{n_b} - \frac{\sum_{l \neq a} W^{(a,l)} 1_{n_l}}{n_a} + \frac{\|D_\delta\| 1_{n_a}}{2n_a} - \frac{z}{2} \left(\frac{1}{n_a} + \frac{1}{n_b} \right) 1_{n_a} \\ &\leq \frac{1}{2} \left(\frac{\|D_\delta\|}{n_a} - z \left(\frac{1}{n_a} + \frac{1}{n_b} \right) \right) 1_{n_a} \end{aligned}$$

where $W^{(a,l)} 1_{n_l} \geq 0$ for all l . Therefore,

$$\|B^{(a,b)} 1_{n_b}\|_\infty \leq \frac{n_b}{2} \left(\frac{\|D_\delta\|}{n_a} - z \left(\frac{1}{n_a} + \frac{1}{n_b} \right) \right) \leq \frac{1}{2} (\tau \|D_\delta\| - (\tau + 1)z)$$

since $z \leq 0$ and $0 < \frac{n_b}{n_a} \leq \tau$. Summing over $1 \leq b \leq k$ and using $B^{(a,a)} = 0$, there holds

$$\|B\|_\infty \leq \max_{1 \leq a \leq k} \sum_{b=1}^k \|B^{(a,b)} 1_{n_b}\|_\infty \leq \frac{k-1}{2} (\tau \|D_\delta\| - (\tau + 1)z)$$

where the first equality comes from $B \geq 0$. Note that B is symmetric and nonnegative, and thus by Gershgorin's theorem (Theorem 6.1), the operator norm of B is bounded by its largest eigenvalue in magnitude which is smaller than $\|B\|_\infty$ for nonnegative matrices. Thus

$$\|B\| \leq \|B\|_\infty \leq \frac{k-1}{2} (\tau \|D_\delta\| - (\tau + 1)z).$$

By putting the estimation of $\|B\|$ and (6.27) together into (6.26), we have

$$\begin{aligned} v^\top Qv &\geq \Pi_1 - \Pi_2 + z \geq \min_{1 \leq a \leq k} \lambda_2(L_{\text{iso}}^{(a,a)}) - \frac{k-1}{2}(\tau\|D_\delta\| - (\tau+1)z) + z \\ &\geq \min_{1 \leq a \leq k} \lambda_2(L_{\text{iso}}^{(a,a)}) + \left(\frac{(k-1)(\tau+1)}{2} + 1 \right) z - \frac{(k-1)\tau}{2}\|D_\delta\|. \end{aligned}$$

Therefore, $Q_{T^\perp} \succeq 0$ if

$$z \geq \frac{(k-1)\tau\|D_\delta\| - 2 \min_{1 \leq a \leq k} \lambda_2(L_{\text{iso}}^{(a,a)})}{(k-1)(\tau+1) + 2}.$$

Based on our previous discussion, such a parameter z exists for (6.17) if

$$\frac{(k-1)\tau\|D_\delta\| - 2 \min_{1 \leq a \leq k} \lambda_2(L_{\text{iso}}^{(a,a)})}{(k-1)(\tau+1) + 2} \leq z \leq -3\|D_\delta\|.$$

which is guaranteed by

$$\|D_\delta\| \leq \frac{\min_{1 \leq a \leq k} \lambda_2(L_{\text{iso}}^{(a,a)})}{2(k-1)(\tau+1) + 3}.$$

□

6.1.4 Proof of Theorem 3.2

Proposition 6.6 (Proof of Theorem 3.2). *Assume we have*

$$\frac{\|P_\delta\|_\infty}{1 - \|P_\delta\|_\infty} \leq \frac{\min_{1 \leq a \leq k} \lambda_2((D_{\text{iso}}^{(a,a)})^{-1} L_{\text{iso}}^{(a,a)})}{2(k-1)(\tau+1) + 3}$$

and B is chosen in (6.18). Let $z = -3\|P_\delta\|$ and then for all $a \neq b$,

$$B^{(a,b)} > 0, \quad Q_{T^\perp} \succeq 0, \tag{6.28}$$

hold simultaneously which certifies X_{ncut} as the unique global minimizer to (3.2).

Proof: In the case of normalized cuts, we pick φ_a , A , and τ according to (6.3),

$$\varphi_a = (D^{(a,a)})^{\frac{1}{2}} 1_{n_a}, \quad A = L_{\text{sym}}, \quad \tau = \frac{\max_l \|\varphi_l\|^2}{\min_l \|\varphi_l\|^2}$$

where $\|\varphi_l\|^2 = 1_{n_l}^\top D^{(l,l)} 1_{n_l} = \text{vol}(\Gamma_l)$.

Step 1: Proof of $B^{(a,b)} > 0$. From the construction of $B^{(a,b)}$ in (6.18), it suffices to show $u_{a,b} > 0$ to ensure $B^{(a,b)} > 0$. Note that the diagonal entries of degree matrix D are strictly positive, and we only need to prove $(D^{(a,a)})^{-\frac{1}{2}} u_{a,b} > 0$ which will be shown true if $z \leq -3\|P_\delta\|_\infty$. We first simplify $(D^{(a,a)})^{-\frac{1}{2}} u_{a,b}$ by using fact $A^{(a,b)} = L_{\text{sym}}^{(a,b)} = (D^{(a,a)})^{-\frac{1}{2}} L^{(a,b)} (D^{(b,b)})^{-\frac{1}{2}}$ and $\varphi_a = (D^{(a,a)})^{\frac{1}{2}} 1_{n_a}$. There holds

$$\begin{aligned} (D^{(a,a)})^{-\frac{1}{2}} u_{a,b} &:= \frac{(D^{(a,a)})^{-1} L^{(a,b)} 1_{n_b}}{\|\varphi_b\|^2} - \frac{(D^{(a,a)})^{-1} L^{(a,a)} 1_{n_a}}{\|\varphi_a\|^2} \\ &+ \frac{1}{2} \left(\frac{1_{n_a}^\top L^{(a,a)} 1_{n_a}}{\|\varphi_a\|^4} - \frac{1_{n_b}^\top L^{(b,b)} 1_{n_b}}{\|\varphi_b\|^4} \right) 1_{n_a} - \frac{z}{2} \left(\frac{1}{\|\varphi_a\|^2} + \frac{1}{\|\varphi_b\|^2} \right) 1_{n_a}. \end{aligned} \tag{6.29}$$

For each term in $(D^{(a,a)})^{-\frac{1}{2}} u_{a,b}$, we have their estimates as follows

$$(D^{(a,a)})^{-1} L^{(a,b)} 1_{n_b} = -(D^{(a,a)})^{-1} W^{(a,b)} 1_{n_b} = -P^{(a,b)} 1_{n_b} \geq -\|P_\delta\|_\infty 1_{n_a}, \tag{6.30}$$

$$(D^{(a,a)})^{-1} L^{(a,a)} 1_{n_a} = (I_{n_a} - P^{(a,a)}) 1_{n_a} = \sum_{l \neq a} P^{(a,l)} 1_{n_l} \leq \|P_\delta\|_\infty 1_{n_a}, \tag{6.31}$$

where $L^{(a,b)} = -W^{(a,b)}$ and $L^{(a,a)} = D^{(a,a)} - W^{(a,a)}$. For the third term of $(D^{(a,a)})^{-\frac{1}{2}}u_{a,b}$ in (6.29), we have

$$0 < 1_{n_a}^\top L^{(a,a)} 1_{n_a} = \sum_{l \neq a} 1_{n_a}^\top W^{(a,l)} 1_{n_l} \leq \|\varphi_a\|^2 \|P_\delta\|_\infty. \quad (6.32)$$

This follows from (6.22) and

$$\sum_{l \neq a} W^{(a,l)} 1_{n_l} = D^{(a,a)} \sum_{l \neq a} (D^{(a,a)})^{-1} W^{(a,l)} 1_{n_l} \leq \|P_\delta\|_\infty \cdot D^{(a,a)} 1_{n_a}$$

because $D^{(a,a)}$ is diagonal and $\|\sum_{l \neq a} (D^{(a,a)})^{-1} W^{(a,l)} 1_{n_l}\|_\infty \leq \|P_\delta\|_\infty$. Plugging all these expressions (6.30), (6.31), and (6.32) into $(D^{(a,a)})^{-\frac{1}{2}}u_{a,b}$ results in

$$\begin{aligned} (D^{(a,a)})^{-\frac{1}{2}}u_{a,b} &\geq -\|P_\delta\|_\infty \left(\frac{1}{\|\varphi_a\|^2} + \frac{1}{\|\varphi_b\|^2} + \frac{1}{2\|\varphi_b\|^2} \right) 1_{n_a} - \frac{z}{2} \left(\frac{1}{\|\varphi_a\|^2} + \frac{1}{\|\varphi_b\|^2} \right) 1_{n_a} \\ &\geq -\|P_\delta\|_\infty \left(\frac{1}{\|\varphi_a\|^2} + \frac{3}{2\|\varphi_b\|^2} \right) 1_{n_a} + \frac{3\|P_\delta\|_\infty}{2} \left(\frac{1}{\|\varphi_a\|^2} + \frac{1}{\|\varphi_b\|^2} \right) 1_{n_a} \\ &\geq \frac{\|P_\delta\|_\infty 1_{n_a}}{2\|\varphi_a\|^2} > 0 \end{aligned}$$

under $z \leq -3\|P_\delta\|_\infty$. Therefore, there holds

$$(D^{(a,a)})^{-\frac{1}{2}}u_{a,b} > 0 \iff u_{a,b} > 0$$

which implies $B^{(a,b)} > 0$ for all $a \neq b$.

Step 2: Proof of $Q_{T^\perp} \succeq 0$. The equations $B^{(a,b)}\varphi_b = \|\varphi_b\|^2 u_{a,b} > 0$ guarantees $Q \in T^\perp$ and thus it suffices to show $Q_{T^\perp} \succeq 0$. We will show the claim is true if

$$z \geq \frac{(k-1)\tau\|P_\delta\|_\infty - 2(1 - \|P_\delta\|_\infty) \min_{1 \leq a \leq k} \lambda_2(L_{\text{rw,iso}}^{(a,a)})}{(k-1)(\tau+1) + 2}.$$

First we project Q to T^\perp and then each projected $Q^{(a,b)}$ obeys

$$\begin{aligned} Q_{T^\perp}^{(a,b)} &= \left(I_{n_a} - \frac{\varphi_a \varphi_a^\top}{\|\varphi_a\|^2} \right) (L_{\text{sym}}^{(a,b)} - B^{(a,b)}) \left(I_{n_b} - \frac{\varphi_b \varphi_b^\top}{\|\varphi_b\|^2} \right), \quad a \neq b, \\ Q_{T^\perp}^{(a,a)} &= \left(I_{n_a} - \frac{\varphi_a \varphi_a^\top}{\|\varphi_a\|^2} \right) (L_{\text{sym}}^{(a,a)} + z I_{n_a}) \left(I_{n_a} - \frac{\varphi_a \varphi_a^\top}{\|\varphi_a\|^2} \right), \quad a = b, \end{aligned}$$

where $Q^{(a,b)}$ can be found in (6.13) and (6.14). Let $v \in \mathbb{R}^N$ be a unit vector in the range of T^\perp and that means its a -th block v_a of v satisfies

$$v_a^\top \varphi_a = v_a^\top (D^{(a,a)})^{\frac{1}{2}} 1_{n_a} = 0, \quad \forall 1 \leq a \leq k.$$

We aim to prove $v^\top Q v \geq 0$ for all such $v \in \mathbb{R}^N$ and $\|v\| = 1$. There holds

$$\begin{aligned} v^\top Q v &= v^\top (L_{\text{sym}} + z I_N - B) v \geq v^\top L_{\text{sym}} v - \|B\| + z \\ &\geq (1 - \|P_\delta\|_\infty) \cdot \min_{1 \leq a \leq k} \lambda_2 \left(L_{\text{rw,iso}}^{(a,a)} \right) - \|B\| + z \end{aligned} \quad (6.33)$$

where $L_{\text{rw,iso}}^{(a,a)} = (D_{\text{iso}}^{(a,a)})^{-1} L_{\text{iso}}^{(a,a)}$. In the inequality (6.33) above, we use the claim that

$$v^\top L_{\text{sym}} v \geq (1 - \|P_\delta\|_\infty) \cdot \min_{1 \leq a \leq k} \lambda_2 \left(L_{\text{rw,iso}}^{(a,a)} \right) \quad (6.34)$$

for any v in the range of T^\perp and $\|v\| = 1$. Now we are going to prove this claim and also control the upper bound of $\|B\|$.

Proof of the claim (6.34): First of all, $v^\top L_{\text{sym}} v$ has its lower bound as

$$\begin{aligned}
v^\top L_{\text{sym}} v &= v^\top D^{-\frac{1}{2}} L D^{-\frac{1}{2}} v \geq v^\top D^{-\frac{1}{2}} (L_{\text{iso}} + L_\delta) D^{-\frac{1}{2}} v \\
&\geq v^\top D^{-\frac{1}{2}} L_{\text{iso}} D^{-\frac{1}{2}} v \geq \sum_{a=1}^k v_a^\top (D^{(a,a)})^{-\frac{1}{2}} L_{\text{iso}}^{(a,a)} (D^{(a,a)})^{-\frac{1}{2}} v_a \\
&\geq \sum_{a=1}^k \lambda_2((D^{(a,a)})^{-\frac{1}{2}} L_{\text{iso}}^{(a,a)} (D^{(a,a)})^{-\frac{1}{2}}) \|v_a\|^2 \\
&\geq \min_{1 \leq a \leq k} \lambda_2((D^{(a,a)})^{-\frac{1}{2}} L_{\text{iso}}^{(a,a)} (D^{(a,a)})^{-\frac{1}{2}}).
\end{aligned}$$

which follows from $L = L_{\text{iso}} + L_\delta$, $L_\delta \succeq 0$ and $v_a \perp (D^{(a,a)})^{\frac{1}{2}} 1_{n_a}$. The second last inequality is ensured by the variational characterization of the second smallest eigenvalue of symmetric matrices. By using the fact that SS^\top and $S^\top S$ always have the same eigenvalues for any square matrix S , then we have

$$\lambda_2((D^{(a,a)})^{-\frac{1}{2}} L_{\text{iso}}^{(a,a)} (D^{(a,a)})^{-\frac{1}{2}}) = \lambda_2((L_{\text{iso}}^{(a,a)})^{\frac{1}{2}} (D^{(a,a)})^{-1} (L_{\text{iso}}^{(a,a)})^{\frac{1}{2}})$$

with $S = (D^{(a,a)})^{-\frac{1}{2}} (L_{\text{iso}}^{(a,a)})^{\frac{1}{2}}$. Moreover, there holds

$$\begin{aligned}
(L_{\text{iso}}^{(a,a)})^{\frac{1}{2}} (D^{(a,a)})^{-1} (L_{\text{iso}}^{(a,a)})^{\frac{1}{2}} &= (L_{\text{iso}}^{(a,a)})^{\frac{1}{2}} (D_{\text{iso}}^{(a,a)})^{-\frac{1}{2}} D_{\text{iso}}^{(a,a)} (D^{(a,a)})^{-1} (D_{\text{iso}}^{(a,a)})^{-\frac{1}{2}} (L_{\text{iso}}^{(a,a)})^{\frac{1}{2}} \\
&\succeq (1 - \|P_\delta\|_\infty) \cdot (L_{\text{iso}}^{(a,a)})^{\frac{1}{2}} (D_{\text{iso}}^{(a,a)})^{-1} (L_{\text{iso}}^{(a,a)})^{\frac{1}{2}}
\end{aligned}$$

where the second inequality follows from $D = D_{\text{iso}} + D_\delta$, $\|D^{-1} D_\delta\| \leq \|P_\delta\|_\infty$, and

$$(D^{(a,a)})^{-1} D_{\text{iso}}^{(a,a)} = I_{n_a} - (D^{(a,a)})^{-1} D_\delta^{(a,a)} \succeq (1 - \|P_\delta\|_\infty) I_{n_a}.$$

Note that both $(L_{\text{iso}}^{(a,a)})^{\frac{1}{2}} (D^{(a,a)})^{-1} (L_{\text{iso}}^{(a,a)})^{\frac{1}{2}}$ and $(L_{\text{iso}}^{(a,a)})^{\frac{1}{2}} (D_{\text{iso}}^{(a,a)})^{-1} (L_{\text{iso}}^{(a,a)})^{\frac{1}{2}}$ have 1_{n_a} in the null space. Thus corresponding their second smallest eigenvalues satisfy

$$\begin{aligned}
\lambda_2((L_{\text{iso}}^{(a,a)})^{\frac{1}{2}} (D^{(a,a)})^{-1} (L_{\text{iso}}^{(a,a)})^{\frac{1}{2}}) &\geq (1 - \|P_\delta\|_\infty) \cdot \lambda_2((L_{\text{iso}}^{(a,a)})^{\frac{1}{2}} (D_{\text{iso}}^{(a,a)})^{-1} (L_{\text{iso}}^{(a,a)})^{\frac{1}{2}}) \\
&= (1 - \|P_\delta\|_\infty) \cdot \lambda_2((D_{\text{iso}}^{(a,a)})^{-\frac{1}{2}} L_{\text{iso}}^{(a,a)} (D_{\text{iso}}^{(a,a)})^{-\frac{1}{2}}) \\
&= (1 - \|P_\delta\|_\infty) \cdot \lambda_2((D_{\text{iso}}^{(a,a)})^{-1} L_{\text{iso}}^{(a,a)}) \\
&= (1 - \|P_\delta\|_\infty) \cdot \lambda_2(L_{\text{rw,iso}}^{(a,a)}),
\end{aligned}$$

which proves the claim.

An upper bound of $\|B\|$: Now we estimate $\|B\|$ under the assumption $B^{(a,b)} > 0$ which is guaranteed by $z \leq -3\|P_\delta\|_\infty$. Note that B is symmetric and thus $\|B\|$ equals its largest eigenvalue in magnitude, i.e.,

$$\|B\| = \max\{\lambda_{\max}(B), \lambda_{\max}(-B)\} = \max\{\lambda_{\max}(D^{-\frac{1}{2}} B D^{\frac{1}{2}}), \lambda_{\max}(-D^{-\frac{1}{2}} B D^{\frac{1}{2}})\}.$$

Note that $D^{-\frac{1}{2}} B D^{\frac{1}{2}}$ is nonnegative and by Gershgorin circle theorem (Theorem 6.1), its largest eigenvalue in magnitude is bounded by $\|D^{-\frac{1}{2}} B D^{\frac{1}{2}}\|_\infty$ which obeys

$$\begin{aligned}
\|D^{-\frac{1}{2}} B D^{\frac{1}{2}}\|_\infty &= \max_{1 \leq a \leq k} \sum_{b \neq a} \|(D^{(a,a)})^{-\frac{1}{2}} B^{(a,b)} (D^{(b,b)})^{\frac{1}{2}} 1_{n_b}\|_\infty \\
&= \max_{1 \leq a \leq k} \sum_{b \neq a} \|(D^{(a,a)})^{-\frac{1}{2}} B^{(a,b)} \varphi_b\|_\infty \\
&= \max_{1 \leq a \leq k} \sum_{b \neq a} \|\varphi_b\|^2 \|(D^{(a,a)})^{-\frac{1}{2}} u_{a,b}\|_\infty
\end{aligned} \tag{6.35}$$

where $B^{(a,b)}\varphi_b = \|\varphi_b\|^2 u_{a,b}$ is given by (6.17). By using (6.29) and (6.32), we have an upper bound for the maximal value of $(D^{(a,a)})^{-\frac{1}{2}}u_{a,b}$:

$$\begin{aligned} (D^{(a,a)})^{-\frac{1}{2}}u_{a,b} &\leq \frac{1_{n_a}^\top L^{(a,a)} 1_{n_a}}{2\|\varphi_a\|^4} 1_{n_a} - \frac{z}{2} \left(\frac{1}{\|\varphi_a\|^2} + \frac{1}{\|\varphi_b\|^2} \right) 1_{n_a} \\ &\leq \frac{\|P_\delta\|_\infty}{2\|\varphi_a\|^2} 1_{n_a} - \frac{z}{2} \left(\frac{1}{\|\varphi_a\|^2} + \frac{1}{\|\varphi_b\|^2} \right) 1_{n_a} \end{aligned}$$

since the first two terms in $(D^{(a,a)})^{-\frac{1}{2}}u_{a,b}$ are non-positive. Under $z \leq -3\|P_\delta\|_\infty$, there holds

$$\|\varphi_b\|^2 \|(D^{(a,a)})^{-\frac{1}{2}}u_{a,b}\|_\infty \leq \frac{\|\varphi_b\|^2}{2} \left(\frac{\|P_\delta\|_\infty}{\|\varphi_a\|^2} - z \left(\frac{1}{\|\varphi_a\|^2} + \frac{1}{\|\varphi_b\|^2} \right) \right) \leq \frac{1}{2} (\tau\|P_\delta\|_\infty - (\tau+1)z).$$

By substituting the estimate above into (6.35), we have an upper bound of $\|B\|$,

$$\|B\| \leq \|D^{-\frac{1}{2}}BD^{\frac{1}{2}}\|_\infty \leq \frac{(k-1)}{2}(\tau\|P_\delta\|_\infty - (\tau+1)z). \quad (6.36)$$

By combining (6.34) and (6.36) with (6.33), the lower bound of $v^\top Qv$ in (6.33) satisfies

$$\begin{aligned} v^\top Qv &\geq (1 - \|P_\delta\|_\infty) \min_{1 \leq a \leq k} \lambda_2(L_{\text{rw,iso}}^{(a,a)}) - \frac{(k-1)}{2}(\tau\|P_\delta\|_\infty - (\tau+1)z) + z \\ &= (1 - \|P_\delta\|_\infty) \min_{1 \leq a \leq k} \lambda_2(L_{\text{rw,iso}}^{(a,a)}) + \left(\frac{(k-1)(\tau+1)}{2} + 1 \right) z - \frac{(k-1)\tau\|P_\delta\|_\infty}{2}. \end{aligned}$$

The nonnegativity of $v^\top Qv$ is guaranteed by

$$z \geq \frac{(k-1)\tau\|P_\delta\|_\infty - 2(1 - \|P_\delta\|_\infty) \min_{1 \leq a \leq k} \lambda_2(L_{\text{rw,iso}}^{(a,a)})}{(k-1)(\tau+1) + 2}.$$

Note that we also require $z \leq -3\|P_\delta\|_\infty$ to ensure $B^{(a,b)} > 0$ and thus

$$-3\|P_\delta\|_\infty \geq z \geq \frac{(k-1)\tau\|P_\delta\|_\infty - 2(1 - \|P_\delta\|_\infty) \min_{1 \leq a \leq k} \lambda_2(L_{\text{rw,iso}}^{(a,a)})}{(k-1)(\tau+1) + 2}$$

is needed to ensure the existence of z . This is implied by

$$\frac{\|P_\delta\|_\infty}{1 - \|P_\delta\|_\infty} \leq \frac{\min_{1 \leq a \leq k} \lambda_2(L_{\text{rw,iso}}^{(a,a)})}{2(k-1)(\tau+1) + 3}$$

which is exactly the assumption in Theorem 3.2. \square

6.2 Proof of Theorem 4.1 and 4.2

We begin with presenting two useful supporting results. The first one is the famous Grönwall's inequality which was proposed by Grönwall in [24] and can be found in [49] as well.

Theorem 6.7 (Grönwall's inequality). *If $g(t)$ is nonnegative and $f(t)$ satisfies the integral inequality*

$$f(t) \leq f(t_0) + \int_{t_0}^t g(s)f(s) \, ds, \quad \forall t \geq t_0,$$

then

$$f(t) \leq f(t_0) \exp \left(\int_{t_0}^t g(s) \, ds \right), \quad \forall t \geq t_0.$$

Lemma 6.8. *For a standard Gaussian random variable $g \sim \mathcal{N}(0, 1)$ and $u > 0$, there holds*

$$\mathbb{P}(g \geq u) = \frac{1}{\sqrt{2\pi}} \int_u^\infty e^{-\frac{t^2}{2}} \, dt \leq \frac{1}{2} e^{-\frac{u^2}{2}}.$$

Proof: The proof can be found in [32] but we provide it here for completeness.

$$\begin{aligned}\mathbb{P}(g \geq u) &= \frac{1}{\sqrt{2\pi}} \int_u^\infty e^{-\frac{t^2}{2}} dt = \frac{1}{\sqrt{2\pi}} e^{-\frac{u^2}{2}} \int_u^\infty e^{-\frac{t^2-u^2}{2}} dt \\ &\leq \frac{1}{\sqrt{2\pi}} e^{-\frac{u^2}{2}} \int_u^\infty e^{-\frac{(t-u)^2}{2}} dt = \frac{1}{2} e^{-\frac{u^2}{2}}\end{aligned}$$

where $t^2 - u^2 \geq (t - u)^2$ for $t \geq u > 0$. \square

6.2.1 Proof of Theorem 4.1: Two concentric circles

To prove Theorem 4.1 via Theorem 3.1, we need two quantities: a lower bound for the second smallest eigenvalue of the Laplacian generated from $\{x_{1,i}\}_{i=1}^n$ and $\{x_{2,j}\}_{j=1}^m$ respectively which characterizes the within-cluster connectivity; and an upper bound of $\|D_\delta\|$ which quantifies the inter-cluster connectivity. We first give a lower bound for the graph Laplacian generated from data on a single circle with Gaussian kernel.

Lemma 6.9. *Suppose n data points (with $n \geq 7$) are equi-spaced on a circle with radius r . Let*

$$\sigma^2 = \frac{16r^2\gamma}{n^2 \log(\frac{n}{2\pi})}$$

and the second smallest eigenvalue of the associated graph Laplacian $L = D - W$ satisfies

$$\lambda_2(L) \gtrsim \left(\frac{2\pi}{n}\right)^{\frac{1}{2\gamma}+2} = \left(\frac{2\pi}{n}\right)^{\frac{8r^2}{\sigma^2 n^2 \log(\frac{n}{2\pi})}+2}, \quad \forall \gamma > 0.$$

Note that the lower bound in Lemma 6.9 is not tight at all. Fortunately, it will not affect our performance bound too much. With Lemma 6.9, we are ready to prove Theorem 4.1.

Proof of Theorem 4.1. Suppose the data satisfy (4.1) and consider the associated weight matrix

$$W = \begin{bmatrix} W^{(1,1)} & W^{(1,2)} \\ W^{(2,1)} & W^{(2,2)} \end{bmatrix} \in \mathbb{R}^{(n+m) \times (n+m)}$$

where $\kappa = \frac{r_2}{r_1} > 1$ and $m = \lfloor n\kappa \rfloor > n$. To apply Theorem 3.1, we should estimate $\lambda_2(L_{\text{iso}}^{(a,a)})$ where

$$L_{\text{iso}}^{(a,a)} = \text{diag}(W^{(a,a)} 1_{n_a}) - W^{(a,a)}, \quad a = 1, 2,$$

with $n_1 = n$ and $n_2 = m$, and the inter-cluster connectivity $\|W^{(1,2)} 1_m\|_\infty$ and $\|W^{(2,1)} 1_n\|_\infty$. Note that the distance between two points in different clusters is always greater than $r_2 - r_1$. As a result, every entry in $W^{(1,2)}$ is bounded by $e^{-\frac{(r_1-r_2)^2}{2\sigma^2}}$ where the bandwidth σ is chosen as

$$\sigma^2 = \frac{16r_1^2\gamma}{n^2 \log(\frac{m}{2\pi})}. \quad (6.37)$$

The inter-cluster connectivity is bounded by

$$\begin{aligned}\|D_\delta\| &= \max\{\|W^{(1,2)} 1_m\|_\infty, \|W^{(2,1)} 1_n\|_\infty\} \leq m e^{-\frac{(r_1-r_2)^2}{2\sigma^2}} \\ &= m e^{-\frac{n^2(\kappa-1)^2 \log(\frac{m}{2\pi})}{32\gamma}} = m \left(\frac{2\pi}{m}\right)^{\frac{n^2\Delta^2}{32\gamma}}\end{aligned}$$

where $\Delta = \kappa - 1 = \frac{r_2-r_1}{r_1}$.

By Lemma 6.9 and the σ^2 in (6.37), the second smallest eigenvalue of $L_{\text{iso}}^{(a,a)}$ satisfies

$$\lambda_2(L_{\text{iso}}^{(1,1)}) \gtrsim \left(\frac{2\pi}{n}\right)^{\frac{\log(\frac{m}{2\pi})}{2\gamma \log(\frac{m}{2\pi})}+2} \geq \left(\frac{2\pi}{m}\right)^{\frac{1}{2\gamma}} \frac{4\pi^2}{n^2}, \quad \lambda_2(L_{\text{iso}}^{(2,2)}) \gtrsim \left(\frac{2\pi}{m}\right)^{\frac{1}{2\gamma}+2}$$

where $\frac{n}{r_1} \approx \frac{m}{r_2}$. Since $m > n$, the lower bound for $\min_{a=1,2} \lambda_2(L_{\text{iso}}^{(a,a)})$ satisfies

$$\min_{a=1,2} \lambda_2(L_{\text{iso}}^{(a,a)}) \gtrsim \left(\frac{2\pi}{m}\right)^{\frac{1}{2\gamma}+2}.$$

Under the separation condition of Theorem 4.1,

$$\Delta^2 \geq \frac{16}{n^2} + \frac{32\gamma}{n^2} \left(2 + \frac{\log(7\kappa m)}{\log(\frac{m}{2\pi})}\right),$$

there holds

$$\|D_\delta\| \leq m \left(\frac{2\pi}{m}\right)^{\frac{n^2 \Delta^2}{32\gamma}} \leq m \left(\frac{2\pi}{m}\right)^{\frac{1}{2\gamma}+2+\frac{\log(7\kappa m)}{\log(\frac{m}{2\pi})}} \leq \frac{1}{7\kappa} \left(\frac{2\pi}{m}\right)^{\frac{1}{2\gamma}+2} \lesssim \frac{\min_{a=1,2} \lambda_2(L_{\text{iso}}^{(a,a)})}{2\kappa + 5}$$

where $\kappa > 1$ and $\frac{2\pi}{m} < 1$. As a consequence of Theorem 3.1, the exact recovery via (3.1) is guaranteed under the conditions stated in Theorem 4.1. \square

Proof of Lemma 6.9. Let $x_i = r \begin{bmatrix} \cos(\frac{2\pi i}{n}) \\ \sin(\frac{2\pi i}{n}) \end{bmatrix}$ with $1 \leq i \leq n$. The weight w_{ij} obeys

$$w_{ij} = e^{-\frac{\|x_i - x_j\|^2}{2\sigma^2}} = e^{-\frac{r^2}{\sigma^2} \left(1 - \cos\left(\frac{2(i-j)\pi}{n}\right)\right)} = e^{-\frac{2r^2}{\sigma^2} \sin^2\left(\frac{(i-j)\pi}{n}\right)}$$

where $\|x_i - x_j\|^2 = 2r^2(1 - \cos(\frac{2(i-j)\pi}{n})) = 4r^2 \sin^2(\frac{(i-j)\pi}{n})$.

The key to this estimation is the fact that when σ^2 is small, $\tilde{L} := e^{\frac{2r^2}{\sigma^2} \sin^2(\frac{\pi}{n})} L$ is very close to L_0 where

$$L_0 = \begin{bmatrix} 2 & -1 & 0 & \cdots & 0 & -1 \\ -1 & 2 & -1 & \cdots & 0 & 0 \\ 0 & -1 & 2 & \cdots & 0 & 0 \\ \vdots & \vdots & \vdots & \ddots & \vdots & \vdots \\ 0 & 0 & 0 & \cdots & 2 & -1 \\ -1 & 0 & 0 & \cdots & -1 & 2 \end{bmatrix}$$

which is the graph Laplacian of an n -cycle. We write down the explicit formula for each entry of \tilde{L} as

$$\tilde{L}_{ij} = \begin{cases} -e^{\frac{2r^2}{\sigma^2} \left(\sin^2(\frac{\pi}{n}) - \sin^2(\frac{(i-j)\pi}{n})\right)}, & \text{if } i \neq j, \\ 2 + e^{\frac{2r^2}{\sigma^2} \sin^2(\frac{\pi}{n})} \sum_{l=2}^{n-2} e^{-\frac{2r^2}{\sigma^2} \sin^2(\frac{\pi l}{n})}, & \text{if } i = j. \end{cases}$$

From Weyl's Inequality in [41], we have

$$\lambda_2(\tilde{L}) \geq \lambda_2(L_0) - \|\tilde{L} - L_0\|.$$

In fact, $\tilde{L} - L_0$ is also a graph Laplacian generated from the weight matrix with (i, j) -entry $e^{\frac{2r^2}{\sigma^2} \sin^2(\frac{\pi}{n})} w_{ij} \cdot 1_{\{2 \leq |i-j| \leq n-2\}}$. Thus, the operator norm of $\tilde{L} - L_0$ is bounded by twice the maximal degree, i.e.,

$$\|\tilde{L} - L_0\| \leq 2e^{\frac{2r^2}{\sigma^2} \sin^2(\frac{\pi}{n})} \sum_{l=2}^{n-2} e^{-\frac{2r^2}{\sigma^2} \sin^2(\frac{\pi l}{n})} \leq 4e^{\frac{2r^2}{\sigma^2} \sin^2(\frac{\pi}{n})} \sum_{l=2}^{\lfloor \frac{n}{2} \rfloor} e^{-\frac{2r^2}{\sigma^2} \sin^2(\frac{\pi l}{n})}$$

because of the Gershgorin circle theorem and the symmetry of $\tilde{L} - L_0$.

Note that $\frac{2x}{\pi} \leq \sin(x) \leq x$ for $0 \leq x \leq \frac{\pi}{2}$, and then

$$\begin{aligned} \|\tilde{L} - L_0\| &\leq 4e^{\frac{2r^2\pi^2}{n^2\sigma^2}} \sum_{l=2}^{\lfloor \frac{n}{2} \rfloor} e^{-\frac{8r^2l^2}{n^2\sigma^2}} \leq 4e^{\frac{2r^2\pi^2}{n^2\sigma^2}} \left(e^{-\frac{32r^2}{n^2\sigma^2}} + \int_2^\infty e^{-\frac{8r^2t^2}{n^2\sigma^2}} dt \right) \\ &= 4e^{\frac{2r^2(\pi^2-16)}{n^2\sigma^2}} + \frac{n\sigma}{r} e^{\frac{2r^2\pi^2}{n^2\sigma^2}} \int_{\frac{8r}{n\sigma}}^\infty e^{-\frac{s^2}{2}} ds \\ &\leq \left(4 + \frac{n\sigma}{r} \sqrt{\frac{\pi}{2}} \right) e^{\frac{2r^2(\pi^2-16)}{n^2\sigma^2}}, \end{aligned}$$

where $s = \frac{4rt}{n\sigma}$; the second inequality is due to the monotonicity of the Gaussian kernel, and the last inequality follows from Lemma 6.8.

Note that $\lambda_2(L_0) = 2 - 2\cos\left(\frac{2\pi}{n}\right)$, see [16, Chapter 1], and hence

$$\lambda_2(\tilde{L}) \geq 2 - 2\cos\left(\frac{2\pi}{n}\right) - \left(4 + \frac{n\sigma}{r} \sqrt{\frac{\pi}{2}} \right) e^{\frac{2r^2(\pi^2-16)}{n^2\sigma^2}} \gtrsim \frac{4\pi^2}{n^2} - \left(4 + \frac{n\sigma}{r} \sqrt{\frac{\pi}{2}} \right) e^{\frac{2r^2(\pi^2-16)}{n^2\sigma^2}}.$$

Now we substitute $\sigma^2 = \frac{16r^2\gamma}{n^2 \log(\frac{n}{2\pi})}$ back into $\lambda_2(\tilde{L})$, and by definition of \tilde{L} , the second smallest eigenvalue of L satisfies

$$\begin{aligned} \lambda_2(L) &= e^{-\frac{2r^2}{\sigma^2} \sin^2(\frac{\pi}{n})} \lambda_2(\tilde{L}) \geq e^{-\frac{8r^2}{n^2\sigma^2}} \lambda_2(\tilde{L}) \gtrsim \left(\frac{2\pi}{n} \right)^{\frac{1}{2\gamma}} \left(\frac{4\pi^2}{n^2} - \left(4 + \frac{n\sigma}{r} \sqrt{\frac{\pi}{2}} \right) e^{\frac{2r^2(\pi^2-16)}{n^2\sigma^2}} \right) \\ &\geq \left(\frac{2\pi}{n} \right)^{\frac{1}{2\gamma}} \left(\frac{4\pi^2}{n^2} - \left(4 + 2\sqrt{\frac{2\pi\gamma}{\log(\frac{n}{2\pi})}} \right) \left(\frac{2\pi}{n} \right)^{\frac{3}{4\gamma}} \right). \end{aligned}$$

By letting $0 < \gamma \leq \frac{1}{4}$, we have

$$\lambda_2(L) \gtrsim \left(\frac{2\pi}{n} \right)^{\frac{1}{2\gamma}+2}. \quad (6.38)$$

So far, we have established a lower bound of $\lambda_2(L)$ for small $\gamma \leq \frac{1}{4}$ (or small σ^2 equivalently). Now we extend this bound for any $\gamma > 0$. Let $L(t)$ be the graph Laplacian w.r.t. the weight matrix $W(t)$ whose (i, j) -entry is $w_{ij}(t) = e^{-\frac{2r^2}{t} \sin^2(\frac{(i-j)\pi}{n})}$ and the derivative of each $w_{ij}(t)$ obeys

$$\begin{aligned} \frac{dw_{ij}(t)}{dt} &= \frac{2r^2}{t^2} \sin^2\left(\frac{(i-j)\pi}{n}\right) w_{ij}(t) \\ &\geq \frac{2r^2}{t^2} \cdot \frac{4}{\pi^2} \cdot \frac{\pi^2}{n^2} w_{ij}(t) = \frac{8r^2}{n^2 t^2} w_{ij}(t) > 0, \quad \text{if } i \neq j. \end{aligned} \quad (6.39)$$

Note that $L(t) = \text{diag}(W(t)1_N) - W(t)$ and by fundamental theorem of calculus, we have

$$L(t) = \int_{t_0}^t \frac{dL(s)}{ds} ds + L(t_0)$$

where $\frac{dL(t)}{dt}$ is also a graph Laplacian w.r.t. the weight matrix $\frac{dw_{ij}(t)}{dt}$. For given t , let v be the normalized eigenvector w.r.t. the second smallest eigenvalue of $L(t)$, then

$$\begin{aligned} \lambda_2(L(t)) &= v^\top L(t) v = \int_{t_0}^t v^\top \left(\frac{dL(s)}{ds} \right) v ds + v^\top L(t_0) v \\ &\geq \frac{8r^2}{n^2} \int_{t_0}^t \frac{v^\top (L(s) v)}{s^2} ds + \lambda_2(L(t_0)) \\ &\geq \frac{8r^2}{n^2} \int_{t_0}^t \frac{\lambda_2(L(s))}{s^2} ds + \lambda_2(L(t_0)) \end{aligned}$$

where the first inequality follows from the quadratic form of graph Laplacian (2.5) and (6.39),

$$v^\top \left(\frac{dL(s)}{ds} \right) v = \sum_{i < j} \frac{dw_{ij}(s)}{ds} (v_i - v_j)^2 \geq \frac{8r^2}{n^2 s^2} \sum_{i < j} w_{ij}(s) (v_i - v_j)^2 = \frac{8r^2}{n^2 s^2} v^\top L(s) v.$$

By Grönwall's inequality, i.e., Theorem 6.7, with $f(t) = -\lambda_2(L(t))$ and $g(t) = \frac{8r^2}{n^2 t^2}$,

$$\lambda_2(L(t)) \geq \lambda_2(L(t_0)) e^{\frac{8r^2}{n^2} \int_{t_0}^t \frac{1}{s^2} ds} = \lambda_2(L(t_0)) e^{-\frac{8r^2}{n^2} \left(\frac{1}{t} - \frac{1}{t_0} \right)}.$$

Finally, we let $t = \sigma^2 = \frac{16r^2 \gamma}{n^2 \log(\frac{n}{2\pi})}$ with $\gamma \geq \frac{1}{4}$ and $t = \sigma_0^2$ with $\gamma_0 = \frac{1}{4}$ ($\sigma \geq \sigma_0$). Then by substituting these parameters into the estimation above and applying (6.38), the Fiedler eigenvalue of $L(\sigma^2)$ satisfies

$$\lambda_2(L(\sigma^2)) \geq \lambda_2(L(\sigma_0^2)) \left(\frac{2\pi}{n} \right)^{\frac{1}{2\gamma} - \frac{1}{2\gamma_0}} = \left(\frac{2\pi}{n} \right)^{\frac{1}{2\gamma_0} + 2} \left(\frac{2\pi}{n} \right)^{\frac{1}{2\gamma} - \frac{1}{2\gamma_0}} = \left(\frac{2\pi}{n} \right)^{\frac{1}{2\gamma} + 2}$$

for any $\gamma > 0$. □

6.2.2 Proof of Theorem 4.2: Two parallel lines

We first estimate the second smallest eigenvalue of the graph Laplacian of one single cluster and then apply Theorem 3.1.

Lemma 6.10. *Suppose there are n equispaced points on the unit interval and the weight matrix W is constructed via Gaussian kernel with $\sigma^2 = \frac{\gamma}{(n-1)^2 \log(\frac{n}{\pi})}$. The second smallest eigenvalue of graph Laplacian $L = D - W$ satisfies*

$$\lambda_2(L) \gtrsim \left(\frac{\pi}{n} \right)^{\frac{1}{2\gamma} + 2}, \quad \gamma > 0. \quad (6.40)$$

Proof of Theorem 4.2. Note that the any two points on different lines are separated by at least Δ . Under

$$\Delta^2 \geq 6\sigma^2 \log n + \frac{1}{(n-1)^2}, \quad \sigma^2 = \frac{\gamma}{(n-1)^2 \log(\frac{n}{\pi})}$$

there holds

$$\|D_\delta\| \leq n e^{-\frac{\Delta^2}{2\sigma^2}} \leq n e^{-\left(3 \log n + \frac{1}{2\sigma^2(n-1)^2}\right)} = e^{-\left(2 \log n + \frac{1}{2\sigma^2(n-1)^2}\right)}.$$

Then we apply Lemma 6.10 and get

$$\min_{a=1,2} \lambda_2(L_{\text{iso}}^{(a,a)}) \gtrsim \left(\frac{\pi}{n} \right)^{\frac{1}{2\gamma} + 2} = e^{-\left(\frac{1}{2\gamma} + 2\right) \log\left(\frac{n}{\pi}\right)} = e^{-\left(2 \log\left(\frac{n}{\pi}\right) + \frac{1}{2\sigma^2(n-1)^2}\right)}.$$

Thus, exact recovery is guaranteed since the assumptions of Theorem 3.1 are fulfilled,

$$\|D_\delta\| \leq e^{-\left(2 \log n + \frac{1}{2\sigma^2(n-1)^2}\right)} \leq \frac{1}{7} \cdot e^{-\left(2 \log\left(\frac{n}{\pi}\right) + \frac{1}{2\sigma^2(n-1)^2}\right)} \lesssim \frac{1}{7} \min_{a=1,2} \lambda_2(L_{\text{iso}}^{(a,a)}).$$

□

Proof of Lemma 6.10. For each cluster in (4.3), its weight matrix is a Toeplitz matrix and satisfies

$$w_{ij} = e^{-\frac{|i-j|^2}{2\sigma^2(n-1)^2}}, \quad 1 \leq i, j \leq n, \quad (6.41)$$

with Gaussian kernel $\Phi_\sigma(x, y) = e^{-\frac{\|x-y\|^2}{2\sigma^2}}$.

The proof strategy is similar to that of Lemma 6.9. We first show the lower bound of the Fiedler eigenvalue (6.40) holds for $\gamma \leq \frac{1}{2}$ and later extend this to any $\gamma > 0$. We claim that $\tilde{L} := e^{\frac{1}{2\sigma^2(n-1)^2}} L$ is very close to L_0 if σ^2 is small, where

$$L_0 = \begin{bmatrix} 1 & -1 & 0 & \cdots & 0 & 0 \\ -1 & 2 & -1 & \cdots & 0 & 0 \\ 0 & -1 & 2 & \cdots & 0 & 0 \\ \vdots & \vdots & \vdots & \ddots & \vdots & \vdots \\ 0 & 0 & 0 & \cdots & 2 & -1 \\ 0 & 0 & 0 & \cdots & -1 & 1 \end{bmatrix}$$

which is the graph Laplacian of a path of n nodes. Note that $\lambda_2(L_0)$ is given explicitly by $\lambda_2(L_0) = 2 - 2 \cos\left(\frac{\pi}{n}\right)$, also see [16, Chapter 1]. All the entries in \tilde{L} are of the following form:

$$\tilde{L}_{ij} = \begin{cases} -e^{\frac{1-|i-j|^2}{2\sigma^2(n-1)^2}}, & \text{if } i \neq j, \\ 2 + e^{\frac{1}{2\sigma^2(n-1)^2}} \sum_{l:|l-i|\geq 2} e^{\frac{-|i-l|^2}{2\sigma^2(n-1)^2}}, & \text{if } i = j, \text{ and } i \neq 1 \text{ or } n, \\ 1 + e^{\frac{1}{2\sigma^2(n-1)^2}} \sum_{l:|l-i|\geq 2} e^{\frac{-|i-l|^2}{2\sigma^2(n-1)^2}}, & \text{if } i = j, \text{ and } i = 1 \text{ or } n. \end{cases}$$

Still, by Weyl's Inequality in [41], the second smallest eigenvalue of \tilde{L} satisfies

$$\lambda_2(\tilde{L}) \geq \lambda_2(L_0) - \|\tilde{L} - L_0\|.$$

To have a lower bound for $\lambda_2(\tilde{L})$, it suffices to get an upper bound for $\|\tilde{L} - L_0\|$. Note $\tilde{L} - L_0$ is also a graph Laplacian generated from the weight matrix whose (i, j) -entry is $e^{\frac{1}{2\sigma^2(n-1)^2}} w_{ij} \cdot 1_{\{|i-j|\geq 2\}}$. Thus, the operator norm of $\tilde{L} - L_0$ is bounded by twice the maximal degree of the weight matrix $\{e^{\frac{1}{2\sigma^2(n-1)^2}} w_{ij} \cdot 1_{\{|i-j|\geq 2\}}\}$. Therefore, the operator norm of $\tilde{L} - L_0$ satisfies

$$\|\tilde{L} - L_0\| \leq 4e^{\frac{1}{2\sigma^2(n-1)^2}} \sum_{l=2}^{\lfloor \frac{n+1}{2} \rfloor} e^{-\frac{l^2}{2\sigma^2(n-1)^2}} \leq 4e^{\frac{1}{2\sigma^2(n-1)^2}} \sum_{l=2}^{\infty} e^{-\frac{l^2}{2\sigma^2(n-1)^2}}.$$

This is also due to Gershgorin circle theorem, see Theorem 6.1, as well as the symmetry of $\tilde{L} - L_0$. By using Lemma 6.8, we immediately have an upper bound of $\|\tilde{L} - L_0\|$ as follows

$$\begin{aligned} \|\tilde{L} - L_0\| &\leq 4e^{\frac{1}{2\sigma^2(n-1)^2}} \sum_{l=2}^{\infty} e^{-\frac{l^2}{2\sigma^2(n-1)^2}} \\ &\leq 4e^{\frac{1}{2\sigma^2(n-1)^2}} \left(e^{-\frac{2}{\sigma^2(n-1)^2}} + \int_2^{\infty} e^{-\frac{t^2}{2\sigma^2(n-1)^2}} dt \right) \\ &= 4e^{-\frac{3}{2\sigma^2(n-1)^2}} + 4\sigma(n-1)e^{\frac{1}{2\sigma^2(n-1)^2}} \int_{\frac{2}{\sigma(n-1)}}^{\infty} e^{-\frac{s^2}{2}} ds \\ &\leq \left(4 + 2\sqrt{2\pi}\sigma(n-1) \right) e^{-\frac{3}{2\sigma^2(n-1)^2}} \end{aligned}$$

where $s = \frac{t}{\sigma(n-1)}$. Hence,

$$\begin{aligned} \lambda_2(\tilde{L}) &\geq 2 - 2 \cos\left(\frac{\pi}{n}\right) - \left(4 + 2\sqrt{2\pi}\sigma(n-1) \right) e^{-\frac{3}{2\sigma^2(n-1)^2}} \\ &\gtrsim \frac{\pi^2}{n^2} - \left(4 + 2\sqrt{2\pi}\sigma(n-1) \right) e^{-\frac{3}{2\sigma^2(n-1)^2}}. \end{aligned}$$

Note $\sigma^2 = \frac{\gamma}{(n-1)^2 \log(\frac{n}{\pi})}$ and there holds

$$\begin{aligned}\lambda_2(L) &= e^{-\frac{1}{2\sigma^2(n-1)^2}} \lambda_2(\tilde{L}) \gtrsim e^{-\frac{\log(\frac{n}{\pi})}{2\gamma}} \left(\frac{\pi^2}{n^2} - \left(4 + 2\sqrt{\frac{2\pi\gamma}{\log(\frac{n}{\pi})}} \right) \left(\frac{\pi}{n} \right)^{\frac{3}{2\gamma}} \right) \\ &= \left(\frac{\pi}{n} \right)^{\frac{1}{2\gamma}} \left(\frac{\pi^2}{n^2} - \left(4 + 2\sqrt{\frac{2\pi\gamma}{\log(\frac{n}{\pi})}} \right) \left(\frac{\pi}{n} \right)^{\frac{3}{2\gamma}} \right).\end{aligned}$$

To ensure that $\lambda_2(L)$ has a non-trivial lower bound, we pick $\gamma \leq \frac{1}{2}$ and then

$$\lambda_2(L) \gtrsim \left(\frac{\pi}{n} \right)^{\frac{1}{2\gamma} + 2}.$$

Now we extend γ to \mathbb{R}_+ . It is not hard to see that $\lambda_2(L)$ (if you treat the weight as a function of bandwidth σ) is an increasing function of σ^2 because the larger σ^2 is, the more connected the graph becomes. Define $L(t)$ to be the Laplacian matrix associated with $W(t) = (w_{ij}(t))_{ij}$ where $w_{ij} = e^{-\frac{|i-j|^2}{2(n-1)^2 t}}$. There holds

$$\frac{dw_{ij}(t)}{dt} = \frac{|i-j|^2}{2(n-1)^2 t^2} e^{-\frac{|i-j|^2}{2(n-1)^2 t}} \geq \frac{1}{2(n-1)^2 t^2} e^{-\frac{|i-j|^2}{2(n-1)^2 t}}, \quad i \neq j. \quad (6.42)$$

Then

$$L(t) = \int_{t_0}^t \frac{dL(s)}{ds} ds + L(t_0)$$

where $\frac{dL(s)}{ds}$ denotes the Laplacian matrix generated by the weight $\left(\frac{dw_{ij}(s)}{ds} \right)_{1 \leq i, j \leq n}$. Therefore, the three matrices $L(t)$, $L(t_0)$, and $\frac{dL(s)}{ds}$ are all graph Laplacians and have the constant function in their nullspace.

We apply $\lambda_2(\cdot)$ to both sides of the equation above, and then the following relation holds

$$\lambda_2(L(t)) \geq \int_{t_0}^t \lambda_2 \left(\frac{dL(s)}{ds} \right) ds + \lambda_2(L(t_0)) \quad (6.43)$$

which follows from the variational form of the second smallest eigenvalue. For $\frac{dL(s)}{ds}$ and $v \perp 1_n$, there holds

$$\begin{aligned}v^\top \left(\frac{dL(s)}{ds} \right) v &= \sum_{i < j} \frac{dw_{ij}(s)}{ds} (v_i - v_j)^2 \\ &\geq \frac{1}{2(n-1)^2 s^2} \sum_{i < j} w_{ij}(s) (v_i - v_j)^2 = \frac{1}{2(n-1)^2 s^2} v^\top L(s) v\end{aligned}$$

which follows from (2.5) and (6.42). Hence

$$\lambda_2 \left(\frac{dL(s)}{ds} \right) \geq \frac{1}{2(n-1)^2 s^2} \lambda_2(L(s)).$$

By substituting this expression into (6.43), we have

$$\lambda_2(L(t)) \geq \frac{1}{2(n-1)^2} \int_{t_0}^t \frac{\lambda_2(L(s))}{s^2} ds + \lambda_2(L(t_0)).$$

By applying Grönwall's inequality (Theorem 6.7) with $f(t) = -\lambda_2(L(t))$ and $g(t) = \frac{1}{2(n-1)^2 t^2}$, we obtain

$$\lambda_2(L(t)) \geq \lambda_2(L(t_0)) e^{\frac{1}{2(n-1)^2} \int_{t_0}^t \frac{1}{s^2} ds} = \lambda_2(L(t_0)) e^{\frac{1}{2(n-1)^2} \left(\frac{1}{t_0} - \frac{1}{t} \right)}.$$

So we get a lower bound of $\lambda_2(L(t))$ for all $t > t_0$. Setting $t = \sigma^2$ and $t_0 = \sigma_0^2$ with $t > t_0$, we get

$$\lambda_2(L(\sigma^2)) \geq \lambda_2(L(\sigma_0^2)) \exp \left(\frac{1}{2(n-1)^2} \left(\frac{1}{\sigma_0^2} - \frac{1}{\sigma^2} \right) \right).$$

By letting $\sigma_0^2 = \frac{\gamma_0}{(n-1)^2 \log(\frac{n}{\pi})}$ ($\gamma_0 = \frac{1}{2}$) and using $\lambda_2(L(\sigma_0^2)) \gtrsim \frac{\pi^3}{n^3}$, we see that the second smallest eigenvalue of $L(\sigma^2)$ is bounded by

$$\lambda_2(L(\sigma^2)) \gtrsim \frac{\pi^3}{n^3} \cdot \frac{n}{\pi} \cdot e^{-\frac{1}{2\sigma^2(n-1)^2}} = \frac{\pi^2}{n^2} \cdot e^{-\frac{1}{2\sigma^2(n-1)^2}}.$$

Now set $\sigma^2 = \frac{\gamma}{(n-1)^2 \log(\frac{n}{\pi})}$, which yields

$$\lambda_2(L(\sigma^2)) \gtrsim \left(\frac{\pi}{n} \right)^{\frac{1}{2\gamma} + 2}$$

for any $\gamma > 0$. □

6.3 Proof of Theorem 4.5: Stochastic block model

The proof relies on two ingredients: a lower bound of the second smallest eigenvalue of random graph Laplacian; and an upper bound of $\|D_\delta\|$. Both quantities can be easily obtained via tools in random matrix theory [45] and Bernstein inequality for scalar random variables [46].

Theorem 6.11 (Bernstein inequality). *For a finite sequence of centered independent random variables $\{z_k\}$ with $|z_k| \leq R$, there holds*

$$\mathbb{P} \left(\sum_{k=1}^n z_k \geq t \right) \leq \exp \left(- \frac{t^2/2}{\sum_{k=1}^n \mathbb{E} z_k^2 + \frac{1}{3} R t} \right).$$

Theorem 6.12 (Matrix Chernoff inequality). *Consider a finite sequence $\{Z_k\}$ of independent, random, self-adjoint matrices with dimension n . Assume that each random matrix satisfies*

$$Z_k \succeq 0, \quad \|Z_k\| \leq R.$$

Let $Z = \sum_{k=1}^n Z_k$ and define $\mu_{\min} = \lambda_{\min}(\mathbb{E}(Z))$. Then

$$\mathbb{P}(\lambda_{\min}(Z) \leq (1 - \eta)\mu_{\min}) \leq n \left[\frac{e^{-\eta}}{(1 - \eta)^{1-\eta}} \right]^{\mu_{\min}/R}, \quad 0 \leq \eta \leq 1. \quad (6.44)$$

Remark 6.13. *Instead of using the right hand side of (6.44) directly, one can use the following simpler form,*

$$\frac{e^{-\eta}}{(1 - \eta)^{1-\eta}} \leq e^{-\frac{\eta^2}{2}}, \quad 0 \leq \eta \leq 1.$$

With matrix Chernoff inequality, we present the following lemma for a lower bound of eigengap.

Lemma 6.14. *Let W be an $n \times n$ symmetric random matrix whose (i, j) entry is binary and takes value 1 with probability p . Then the second smallest eigenvalue of its corresponding graph Laplacian satisfies*

$$\mathbb{P}(\lambda_2(L) \geq (1 - \eta)np) \geq 1 - n \exp \left(- \frac{np\eta^2}{4} \right)$$

where $0 < \eta < 1$.

Now we are ready to present the final proof of Theorem 4.5.

Proof of Theorem 4.5. For the stochastic block model with two clusters, the corresponding weight matrix and its expectation are

$$W = \begin{bmatrix} W^{(1,1)} & W^{(1,2)} \\ W^{(2,1)} & W^{(2,2)} \end{bmatrix}, \quad \mathbb{E}(W) = \begin{bmatrix} pJ_{n \times n} & qJ_{n \times n} \\ qJ_{n \times n} & pJ_{n \times n} \end{bmatrix} \in \mathbb{R}^{N \times N}$$

where $N = 2n$. By Lemma 6.14, the graph Laplacian $L_{\text{iso}}^{(a,a)}$ of $W^{(a,a)}$ has its second smallest eigenvalue bounded by

$$\lambda_2(L_{\text{iso}}^{(a,a)}) \geq (1 - \eta)np, \quad a = 1, 2,$$

with probability at least $1 - 2n \exp\left(-\frac{np\eta^2}{4}\right)$. In particular, if we pick $p = \frac{\alpha \log N}{N}$, then $\min \lambda_2(L_{\text{iso}}^{(a,a)}) \geq \frac{(1-\eta)\alpha \log N}{2}$ holds with probability at least $1 - \mathcal{O}(N^{-\epsilon})$ for $\epsilon > 0$ if $\eta^2\alpha > 8$.

Now we take a look at $\|D_\delta\|$ which equals

$$\|D_\delta\| = \max \left\{ \|W^{(1,2)}1_n\|_\infty, \|W^{(2,1)}1_n\|_\infty \right\}.$$

Each diagonal entry of D_δ is a sum of n i.i.d. Bernoulli random variables and each of these random variables takes 1 with probability q . By applying Bernstein inequality and then taking the union bound over all entries in D_δ , we have

$$\mathbb{P}(\|D_\delta\| \leq nq + t) \geq 1 - N \exp\left(-\frac{t^2/2}{nq(1-q) + t/3}\right).$$

To fulfill the assumptions in Theorem 3.1, we need $nq + t \leq \frac{(1-\eta)np}{7} \leq \frac{\min \lambda_2(L_{\text{iso}}^{(a,a)})}{7}$ and it suffices to have $t \leq \frac{(1-\eta)np}{7} - nq = \frac{1}{2} \left(\frac{(1-\eta)\alpha}{7} - \beta \right) \log N$ where $q = \frac{\beta \log N}{N}$. Substituting these estimations into the formula above results in

$$\mathbb{P}\left(\|D_\delta\| \leq \frac{\min \lambda_2(L_{\text{iso}}^{(a,a)})}{7}\right) \geq 1 - N \exp\left(-\frac{\left(\frac{(1-\eta)\alpha}{7} - \beta\right)^2 \frac{\log N}{8}}{\frac{\beta}{2} + \frac{1}{6} \left(\frac{(1-\eta)\alpha}{7} - \beta\right)}\right) = 1 - \mathcal{O}(N^{-\epsilon})$$

if we require

$$\left(\frac{(1-\eta)\alpha}{7} - \beta\right)^2 > 4\beta + \frac{4}{3} \left(\frac{(1-\eta)\alpha}{7} - \beta\right), \quad \eta^2\alpha > 8.$$

Note that the first inequality satisfies

$$\frac{(1-\eta)\alpha}{7} - \beta > \frac{2}{3} + 2\sqrt{\frac{1}{9} + \beta} \iff \alpha > \frac{14}{1-\eta} \left(\frac{1}{3} + \frac{\beta}{2} + \sqrt{\frac{1}{9} + \beta}\right).$$

Let $\eta = 0.65$ and we arrive at the desired bound,

$$\alpha > 40 \left(\frac{1}{3} + \frac{\beta}{2} + \sqrt{\frac{1}{9} + \beta}\right)$$

which guarantees the exact recovery of the planted communities. \square

Proof of Lemma 6.14. Suppose W is an $n \times n$ self-adjoint matrix, and each entry w_{ij} is binary and takes value 1 with probability p . Let $\{e_i\}_{i=1}^N$ be the canonical basis in \mathbb{R}^N . Then the graph Laplacian of W is the sum of weighted rank-1 Laplacian matrices,

$$L = \sum_{i < j} w_{ij} L_{ij}, \quad L_{ij} := (e_i - e_j)(e_i - e_j)^\top,$$

which follow from (2.5) directly. By the definition of W , the expectation of L satisfies

$$\mathbb{E}(L) = p \sum_{i < j} L_{ij} = p(nI_n - J_{n \times n}).$$

Hence, there hold $\lambda_2(\mathbb{E}(L)) = np$, $L_{ij} \succeq 0$, and $\|L_{ij}\| \leq 2$. Before applying Theorem 6.12, we need to clarify one thing: the matrix Chernoff inequality estimates the smallest eigenvalue while one cares about the second smallest eigenvalue of L . This discrepancy can be easily resolved since all $\{L_{ij}\}_{i < j}$, L , and $\mathbb{E}(L)$ have 0 as the smallest eigenvalue and 1_n as the corresponding eigenvector. Therefore, when restricted on the complement of 1_n , the matrix Chernoff immediately applies to the second smallest eigenvalue. Thus Theorem 6.12 implies that

$$\mathbb{P}(\lambda_2(L) \leq (1 - \eta)np) \leq n \exp\left(-\frac{np\eta^2}{4}\right) \iff \mathbb{P}(\lambda_2(L) \geq (1 - \eta)np) \geq 1 - n \exp\left(-\frac{np\eta^2}{4}\right).$$

□

Proof of claim (4.5). We will prove that $\lambda_2(D_{\text{iso}} - D_\delta - W + \frac{1}{2}1_N 1_N^\top) > 0$ is ensured by (4.5), i.e., $\min \lambda_2(L_{\text{iso}}^{(a,a)}) > 2\|D_\delta\|$. Let $g := \begin{bmatrix} 1_n \\ -1_n \end{bmatrix}$ which is perpendicular to 1_N . Hence there hold

$$\begin{aligned} \lambda_2(D_{\text{iso}} - D_\delta - W + \frac{1}{2}1_N 1_N^\top) &= \lambda_2\left(\text{diag}(g) \left(L_{\text{iso}} - D_\delta - W_\delta + \frac{1}{2}1_N 1_N^\top\right) \text{diag}(g)\right) \\ &= \lambda_2(L_{\text{iso}} - D_\delta + W_\delta + \frac{1}{2}gg^\top) \end{aligned}$$

which follows from the diagonal-block structure of L_{iso} and D_δ , and the diagonal blocks of W_δ are zero. Note that $L_{\text{iso}} + \frac{1}{2}gg^\top$ and $D_\delta - W_\delta$ share the same null space spanned by 1_N . Moreover, we have

$$\lambda_2(L_{\text{iso}} + \frac{1}{2}gg^\top) = \lambda_3(L_{\text{iso}})$$

because g is in the null space of L_{iso} and $\|\frac{1}{2}gg^\top\| = n$ cannot be equal to $\lambda_2(L_{\text{iso}} + \frac{1}{2}gg^\top)$ since $\|L_{\text{iso}}\| \leq n$ holds.

Hence, by Weyl's inequality and $\|D_\delta - W_\delta\| \leq 2\|D_\delta\|$, there holds

$$\begin{aligned} \lambda_2(D_{\text{iso}} - D_\delta - W + \frac{1}{2}1_N 1_N^\top) &\geq \lambda_2(L_{\text{iso}} + \frac{1}{2}gg^\top) - \|D_\delta - W_\delta\| \\ &= \lambda_3(L_{\text{iso}}) - 2\|D_\delta\| = \min \lambda_2(L_{\text{iso}}^{(a,a)}) - 2\|D_\delta\| > 0. \end{aligned}$$

□

Acknowledgement

S.L. thanks Afonso Bandeira for fruitful discussions on stochastic block models.

References

- [1] E. Abbe. Community detection and stochastic block models: recent developments. *arXiv preprint arXiv:1703.10146*, 2017.
- [2] E. Abbe, A. S. Bandeira, and G. Hall. Exact recovery in the stochastic block model. *IEEE Transactions on Information Theory*, 62(1):471–487, 2016.
- [3] N. Agarwal, A. S. Bandeira, K. Koiliaris, and A. Kolla. Multisection in the stochastic block model using semidefinite programming. In *Compressed Sensing and its Applications*, pages 125–162. Springer, 2017.
- [4] A. A. Amini and E. Levina. On semidefinite relaxations for the block model. *The Annals of Statistics*, 46(1):149–179, 2018.
- [5] S. Arora, S. Rao, and U. Vazirani. Expander flows, geometric embeddings and graph partitioning. *Journal of the ACM (JACM)*, 56(2):5, 2009.

- [6] D. Arthur and S. Vassilvitskii. k-means++: The advantages of careful seeding. In *Proceedings of the Eighteenth Annual ACM-SIAM Symposium on Discrete Algorithms*, pages 1027–1035. Society for Industrial and Applied Mathematics, 2007.
- [7] P. Awasthi, A. S. Bandeira, M. Charikar, R. Krishnaswamy, S. Villar, and R. Ward. Relax, no need to round: Integrality of clustering formulations. In *Proceedings of the 2015 Conference on Innovations in Theoretical Computer Science*, pages 191–200. ACM, 2015.
- [8] P. Awasthi and O. Sheffet. Improved spectral-norm bounds for clustering. In *APPROX-RANDOM*, pages 37–49. Springer, 2012.
- [9] A. S. Bandeira. Random laplacian matrices and convex relaxations. *Foundations of Computational Mathematics*, 18(2):345–379, Apr 2018.
- [10] M. Belkin and P. Niyogi. Laplacian eigenmaps and spectral techniques for embedding and clustering. In *Advances in Neural Information Processing Systems*, pages 585–591, 2002.
- [11] M. Belkin and P. Niyogi. Laplacian eigenmaps for dimensionality reduction and data representation. *Neural Computation*, 15(6):1373–1396, 2003.
- [12] M. Belkin and P. Niyogi. Towards a theoretical foundation for Laplacian-based manifold methods. In *International Conference on Computational Learning Theory*, pages 486–500. Springer, 2005.
- [13] A. Ben-Tal and A. Nemirovski. *Lectures on Modern Convex Optimization: Analysis, Algorithms, and Engineering Applications*. SIAM, 2001.
- [14] J. A. Bondy, U. S. R. Murty, et al. *Graph Theory with Applications*, volume 290. Macmillan London, 1976.
- [15] S. Boyd and L. Vandenberghe. *Convex Optimization*. Cambridge University Press, 2004.
- [16] A. E. Brouwer and W. H. Haemers. *Spectra of Graphs*. Springer Science+Business Media, 2011.
- [17] F. R. Chung. *Spectral Graph Theory*, volume 92. American Mathematical Society, 1997.
- [18] R. R. Coifman and S. Lafon. Diffusion maps. *Applied and Computational Harmonic Analysis*, 21(1):5–30, 2006.
- [19] R. R. Coifman, S. Lafon, A. B. Lee, M. Maggioni, B. Nadler, F. Warner, and S. W. Zucker. Geometric diffusions as a tool for harmonic analysis and structure definition of data: Diffusion maps. *Proceedings of the National Academy of Sciences of the United States of America*, 102(21):7426–7431, 2005.
- [20] C. Davis and W. M. Kahan. The rotation of eigenvectors by a perturbation. iii. *SIAM Journal on Numerical Analysis*, 7(1):1–46, 1970.
- [21] I. S. Dhillon, Y. Guan, and B. Kulis. Kernel k-means: spectral clustering and normalized cuts. In *Proceedings of the Tenth ACM SIGKDD International Conference on Knowledge Discovery and Data Mining*, pages 551–556. ACM, 2004.
- [22] M. P. Do Carmo. *Riemannian Geometry*. Birkhauser, 1992.
- [23] G. H. Golub and C. F. Van Loan. *Matrix Computations*. The Johns Hopkins University Press, 3rd edition, 1996.
- [24] T. H. Grönwall. Note on the derivatives with respect to a parameter of the solutions of a system of differential equations. *Annals of Mathematics*, pages 292–296, 1919.

- [25] L. Hagen and A. B. Kahng. New spectral methods for ratio cut partitioning and clustering. *IEEE Transactions on Computer-Aided Design of Integrated Circuits and Systems*, 11(9):1074–1085, 1992.
- [26] T. Hastie, R. Tibshirani, and J. Friedman. Unsupervised learning. In *The Elements of Statistical Learning*, pages 485–585. Springer, 2009.
- [27] T. Iguchi, D. G. Mixon, J. Peterson, and S. Villar. Probably certifiably correct k-means clustering. *Mathematical Programming*, 165(2):605–642, 2017.
- [28] A. K. Jain. Data clustering: 50 years beyond K-means. *Pattern Recognition Letters*, 31(8):651–666, 2010.
- [29] A. Kumar and R. Kannan. Clustering with spectral norm and the k-means algorithm. In *Foundations of Computer Science (FOCS), 2010 51st Annual IEEE Symposium on*, pages 299–308. IEEE, 2010.
- [30] J. Lei and A. Rinaldo. Consistency of spectral clustering in stochastic block models. *The Annals of Statistics*, 43(1):215–237, 2015.
- [31] D. A. Levin, Y. Peres, and E. L. Wilmer. *Markov Chains and Mixing Times*, volume 107. American Mathematical Society, 2017.
- [32] X. Li, Y. Li, S. Ling, T. Strohmer, and K. Wei. When do birds of a feather flock together? k-means, proximity, and conic programming. *arXiv preprint arXiv:1710.06008*, 2017.
- [33] S. Lloyd. Least squares quantization in PCM. *IEEE Transactions on Information Theory*, 28(2):129–137, 1982.
- [34] D. G. Mixon, S. Villar, and R. Ward. Clustering subgaussian mixtures by semidefinite programming. *Information and Inference: A Journal of the IMA*, page iax001, 2017.
- [35] A. Y. Ng, M. I. Jordan, and Y. Weiss. On spectral clustering: analysis and an algorithm. In *Advances in Neural Information Processing Systems*, pages 849–856, 2002.
- [36] J. Peng and Y. Wei. Approximating k-means-type clustering via semidefinite programming. *SIAM Journal on Optimization*, 18(1):186–205, 2007.
- [37] K. Rohe, S. Chatterjee, and B. Yu. Spectral clustering and the high-dimensional stochastic blockmodel. *The Annals of Statistics*, pages 1878–1915, 2011.
- [38] J. Shi and J. Malik. Normalized cuts and image segmentation. *IEEE Transactions on Pattern Analysis and Machine Intelligence*, 22(8):888–905, 2000.
- [39] A. Singer. From graph to manifold Laplacian: The convergence rate. *Applied and Computational Harmonic Analysis*, 21(1):128–134, 2006.
- [40] A. Singer and H.-T. Wu. Spectral convergence of the connection Laplacian from random samples. *Information and Inference: A Journal of the IMA*, 6(1):58–123, 2016.
- [41] G. W. Stewart. Perturbation theory for the singular value decomposition. Technical Report CS-TR-2539, University of Maryland, Sep 1990.
- [42] M. Tepper, A. M. Sengupta, and D. Chklovskii. Clustering is semidefinitely not that hard: Nonnegative SDP for manifold disentangling. *arXiv preprint arXiv:1706.06028v3*, 2017.
- [43] N. G. Trillos, M. Gerlach, M. Hein, and D. Slepcev. Error estimates for spectral convergence of the graph Laplacian on random geometric graphs towards the Laplace-Beltrami operator. *arXiv preprint arXiv:1801.10108*, 2018.

- [44] N. G. Trillos and D. Slepčev. A variational approach to the consistency of spectral clustering. *Applied and Computational Harmonic Analysis*, 2016.
- [45] J. A. Tropp. User-friendly tail bounds for sums of random matrices. *Foundations of Computational Mathematics*, 12(4):389–434, 2012.
- [46] R. Vershynin. Introduction to the non-asymptotic analysis of random matrices. In Y. C. Eldar and G. Kutyniok, editors, *Compressed Sensing: Theory and Applications*, chapter 5. Cambridge University Press, 2012.
- [47] U. Von Luxburg. A tutorial on spectral clustering. *Statistics and Computing*, 17(4):395–416, 2007.
- [48] U. Von Luxburg, M. Belkin, and O. Bousquet. Consistency of spectral clustering. *The Annals of Statistics*, pages 555–586, 2008.
- [49] W. Walter. *Ordinary Differential Equations*, volume 1(182). Springer Science and Media, 1998.
- [50] E. P. Xing and M. I. Jordan. On semidefinite relaxation for normalized k-cut and connections to spectral clustering. Technical Report UCB/CSD-03-1265, EECS Department, University of California, Berkeley, Jun 2003.
- [51] B. Yan, P. Sarkar, and X. Cheng. Exact recovery of number of blocks in blockmodels. *arXiv preprint arXiv:1705.08580*, 2017.